AEM
Journals.ASM.org

Increasing Avermectin Production in *Streptomyces avermitilis* by Manipulating the Expression of a Novel TetR-Family Regulator and Its Target Gene Product

Wenshuai Liu, Qinling Zhang, Jia Guo,* Zhi Chen, Jilun Li, Ying Wen

State Key Laboratory of Agro-Biotechnology and MOA Key Laboratory of Soil Microbiology, College of Biological Sciences, China Agricultural University, Beijing, China

Avermectins produced by *Streptomyces avermitilis* are commercially important anthelmintic agents. The detailed regulatory mechanisms of avermectin biosynthesis remain unclear. Here, we identified SAV3619, a TetR-family transcriptional regulator designated AveT, to be an activator for both avermectin production and morphological differentiation in *S. avermitilis*. AveT was shown to indirectly stimulate avermectin production by affecting transcription of the cluster-situated activator gene *aveR*. AveT directly repressed transcription of its own gene (*aveT*), adjacent gene *pepD2* (*sav_3620*), *sav_7490* (designated *aveM*), and *sav_7491* by binding to an 18-bp perfect palindromic sequence (CGAAACGKTKYCGTTTCG, where K is T or G and Y is T or C and where the underlining indicates inverted repeats) within their promoter regions. *aveM* (which encodes a putative transmembrane efflux protein belonging to the major facilitator superfamily [MFS]), the important target gene of AveT, had a striking negative effect on avermectin production and morphological differentiation. Overexpression of *aveT* and deletion of *aveM* in wild-type and industrial strains of *S. avermitilis* led to clear increases in the levels of avermectin production. *In vitro* gel-shift assays suggested that C-5–O-B1, the late pathway precursor of avermectin B1, acts as an AveT ligand. Taken together, our findings indicate positive-feedback regulation of *aveT* expression and avermectin production by a late pathway intermediate and provide the basis for an efficient strategy to increase avermectin production in *S. avermitilis* by manipulation of AveT and its target gene product, AveM.

Soil-dwelling species of *Streptomyces* produce about half of currently known antibiotics (including antibacterial, anticancer, anthelmintic, and immunosuppressive agents) during their complex morphological differentiation cycle (1) and have many important medical and commercial applications. Antibiotic biosynthesis is controlled by large gene clusters, usually including cluster-situated regulators (CSRs). These CSRs are at the lowest level of the complex regulatory network for antibiotic biosynthesis and are controlled by various higher-level pleiotropic regulators in response to developmental state, population density, environmental signals, and physiological signals (2–4).

The species *Streptomyces avermitilis* produces avermectins, a series of 16-membered macrocyclic lactones (termed A1a, A1b, A2a, A2b, B1a, B1b, B2a, and B2b) that are excellent anthelmintic agents with high potency, broad-spectrum activity against various arthropod and nematode parasites, and a low level of side effects on the host (5, 6). Of the eight avermectin components, B1a has the highest insecticidal activity (7). Avermectins are a commercially important group of antibiotics with annual worldwide sales of ~$850 million (8) and are widely applied in the agricultural, veterinary, and medical fields. The 82-kb *ave* gene cluster that controls avermectin biosynthesis includes 18 open reading frames (ORFs) (9). The gene *aveR*, located at the left end of the gene cluster, encodes a cluster-situated LuxR family activator essential for transcription of all *ave* structural genes (10, 11). The factors that trigger the transcription of *aveR* and the detailed regulatory mechanisms of avermectin biosynthesis remain unclear. Identification and characterization of the transcriptional regulators involved in avermectin biosynthesis are essential for elucidation of the regulatory networks and for the rational design of new hyperproducer strains through genetic manipulation.

Microbial transcriptional regulators are classified on the basis of sequence similarity and structural and functional criteria into families, which include TetR (12), LuxR (13), LysR (14), AraC/XylS (15), LacI (16), and MarR (17). Of the various families of transcriptional regulators present in the *Streptomyces* genome, TetR-family transcriptional regulators (TFRs) are the most abundant. Certain species have over 100 TFRs, including *S. coelicolor* (153 TFRs), *S. avermitilis* (115 TFRs), and *S. griseus* (104 TFRs) (18). These regulators presumably undergo complex interactions during the complicated life cycles of *Streptomyces*. TFRs have been shown to participate in such important cellular processes as multidrug resistance, antibiotic biosynthesis, morphogenesis, osmotic stress, biofilm formation, catabolic pathways, nitrogen uptake, and pathogenicity (19), but the functions of many of them in *Streptomyces* remain unknown.

TFRs consist of two domains: an N-terminal DNA-binding

Received 17 March 2015 **Accepted** 18 May 2015

Accepted manuscript posted online 22 May 2015

Citation Liu W, Zhang Q, Guo J, Chen Z, Li J, Wen Y. 2015. Increasing avermectin production in *Streptomyces avermitilis* by manipulating the expression of a novel TetR-family regulator and its target gene product. Appl Environ Microbiol 81:5157–5173. doi:10.1128/AEM.00868-15.

Editor: M. A. Elliot

Address correspondence to Ying Wen, wen@cau.edu.cn.

* Present address: Jia Guo, Key Laboratory of Carbohydrate Chemistry and Biotechnology, Ministry of Education, School of Biotechnology, Jiangnan University, Wuxi, China.

Supplemental material for this article may be found at http://dx.doi.org/10.1128/AEM.00868-15.

doi:10.1128/AEM.00868-15

TABLE 1 Strains and plasmids used in this study

Strain or plasmid	Description	Source or reference
Strains		
S. avermitilis		
ATCC 31267	WT strain	Laboratory stock
A-178	An industrial strain	Qilu Pharmaceutical
ΔaveT	*aveT* deletion mutant	This study
CaveT	*aveT*-complemented strain	This study
OaveT	*aveT*-overexpressing strain	This study
OaveT/A-178	*aveT*-overexpressing strain based on A-178	This study
WT/pKC1139	WT strain carrying empty vector pKC1139	This study
WT/pSET152	WT strain carrying empty vector pSET152	This study
ΔaveM	*aveM* deletion mutant	This study
CaveM	*aveM*-complemented strain	This study
OaveM	*aveM*-overexpressing strain	This study
ΔaveM/A-178	*aveM* deletion mutant based on A-178	This study
ΔaveTaveM	*aveT aveM* double deletion mutant	This study
OpepD2	*pepD2*-overexpressing strain	This study
Δaco	*aco* deletion mutant	This study
E. coli		
JM109	General cloning host for plasmid manipulation	Laboratory stock
ET12567	Methylation-deficient strain	33
BL21(DE3)	Host for protein overexpression	Novagen
Plasmids		
pKC1139	Multiple-copy, temperature-sensitive *E. coli-Streptomyces* shuttle vector	48
pSET152	Integrative *E. coli-Streptomyces* shuttle vector	48
pET-28a (+)	Vector for protein overexpression in *E. coli*	Novagen
pJL117	pIJ2925 derivative carrying the *Streptomyces* strong constitutive promoter *ermE*p*	49
pΔaveT	*aveT* deletion vector based on pKC1139	This study
pKC1139-ermp-aveT	*aveT*-overexpressing vector based on pKC1139	This study
pSET152-aveT	*aveT*-complemented vector based on pSET152	This study
pET28-aveT	*aveT*-overexpressing vector based on pET-28a (+)	This study
pΔaveM	*aveM* deletion vector based on pKC1139	This study
pKC1139-ermp-aveM	*aveM*-overexpressing vector based on pKC1139	This study
pSET152-aveM	*aveM*-complemented vector based on pSET152	This study
pKC1139-ermp-pepD2	*pepD2*-overexpressing vector based on pKC1139	This study
pΔaco	*aco* deletion vector based on pKC1139	This study

(DNB) domain that is highly conserved across the family and a C-terminal ligand-binding domain (LBD) that displays broad sequence and structural variation and interacts with a wide variety of ligands (19–21). The majority of TFRs act as homodimeric transcriptional repressors (19); a small number act as activators (22–24) or as dual repressors/activators (25). In most TFRs characterized to date, transcription is regulated by binding of the DNB domain to DNA, and such regulation is blocked by conformational changes upon binding of small molecules to the LBD (21). It appears that TFR ligands are often related to the gene(s) regulated, but the cognate ligands for the vast majority of TFRs are unknown (18, 20).

Among 115 TFRs in *S. avermitilis*, our group has characterized SAV151 (26), SAV576 (27), SAV577 (28), and SAV7471 (homologous to SCO0772 in *S. coelicolor*) (29) to be negative regulators of avermectin production. SAV3818 (homologous to SCO4421) (30) and SAV3703 (AvaR3, a γ-butyrolactone autoregulator receptor) (23) are positive regulators of avermectin production. The other 109 TFRs remain to be characterized. The present study revealed a positive regulatory role of a previously uncharacterized *S. avermitilis* TFR, AveT (SAV3619, homologous to SCO3167), in avermectin production and morphological differentiation. We demonstrate that AveT directly represses transcription of the genes *aveT*, *pepD2* (*sav_3620*, homologous to *sco3168*), *aveM* (*sav_7490*), and *sav_7491* (homologous to *sco5759*) and that C-5–O-B1, the late pathway intermediate of avermectin B1, inhibits binding of AveT to its target genes, thereby regulating *aveT* expression and avermectin production via a positive-feedback mechanism. A novel strategy for increasing the industrial-scale avermectin yield through the overexpression of AveT and deletion of its target gene, *aveM*, is described.

MATERIALS AND METHODS

Strains, plasmids, and growth conditions. The strains and plasmids used in this work are listed in Table 1. *S. avermitilis* wild-type (WT) strain ATCC 31267, an avermectin producer, was grown at 28°C and used for gene disruption and propagation. For both ATCC 31267 and A-178 (an industrial strain that produces only avermectin B), sporulation was achieved on solid YMS medium (31). Liquid YEME medium (32) containing 25% sucrose was used to grow mycelia for protoplast preparation and DNA extraction. Protoplast regeneration medium RM14 was prepared as described by MacNeil and Klapko (33). MM (32) and YMS agar were used for observation of the *S. avermitilis* phenotype. For avermectin production, seed medium and insoluble fermentation medium FM-I were

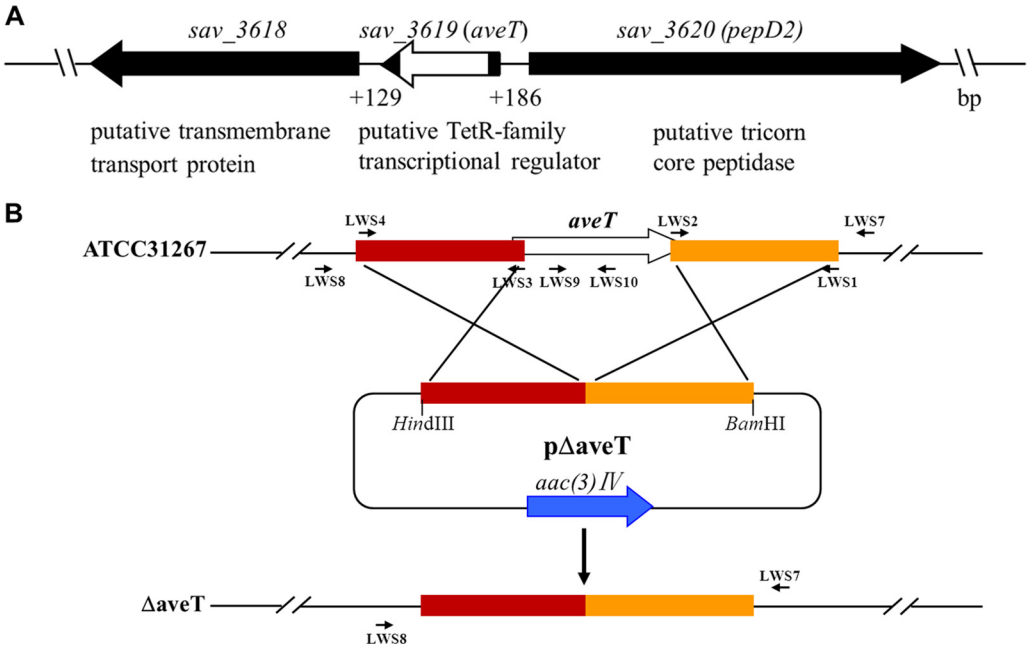

FIG 1 Genetic organization of *aveT* and its adjacent genes in *S. avermitilis* (A) and schematic method used for *aveT* deletion (B). (A) Gene annotations are based on the *S. avermitilis* genome database (http://avermitilis.ls.kitasato-u.ac.jp/). White block, in-frame deletion in *aveT*. (B) Large arrows, genes and their directions; short arrows, primers used for cloning homologous exchange regions and verifying gene deletion (see Materials and Methods); rectangles, exchange regions used for deletion of *aveT*.

used as described previously (34). Soluble fermentation medium FM-II (10) was used to grow mycelia for growth analysis.

Escherichia coli JM109 was used to propagate plasmids for routine cloning. *E. coli* BL21(DE3) (Novagen, Germany) was used as the host for protein overexpression. Nonmethylated DNA was propagated in *E. coli* ET12567 (*dam dcm hsdS*) (33) for transformation into *S. avermitilis*. *E. coli* strains were usually grown in Luria-Bertani (LB) medium at 37°C. The antibiotics were used as described previously by Zhao et al. (35).

Gene deletion, complementation, and overexpression. To construct an *aveT* (*sav_3619*) deletion mutant, two fragments flanking *aveT* were prepared from the genomic DNA of strain ATCC 31267 by PCR. A 596-bp 5′ flanking region (positions −518 to +78 relative to the *aveT* start codon) was amplified with primers LWS4 and LWS3, and a 501-bp 3′ flanking region (positions +524 to +1024) was amplified with primers LWS2 and LWS1. The two fragments were connected by fusion PCR using primers LWS1 and LWS4 and then ligated into HindIII/BamHI-digested pKC1139 to generate *aveT* deletion vector pΔaveT, which was introduced into ATCC 31267 protoplasts. Apramycin-sensitive strains were selected as described previously (35), and the deletion in a mutant with an *aveT* deletion, generated by double-crossover recombination, was confirmed by PCR analysis using primers LWS7, LWS8, LWS9, and LWS10 (Fig. 1B). When using primers LWS7 and LWS8, whose sequences flank the exchange regions, a 1.3-kb band appeared, whereas a 1.7-kb band was detected in the genomic DNA of ATCC 31267. When using primers LWS9 and LWS10, whose sequences are located within the deletion region of *aveT*, only ATCC 31267 produced a 311-bp band, as predicted (data not shown). We thus obtained *aveT* gene deletion mutant ΔaveT, in which *aveT* was mostly deleted (Fig. 1B).

For complementation of strain ΔaveT, a 923-bp DNA fragment carrying the promoter and coding region of *aveT* was amplified from ATCC 31267 with primers LWS11 and LWS12. The PCR product was digested with BamHI/XbaI and then inserted into the corresponding sites of pSET152 to generate *aveT* gene-complemented vector pSET152-aveT, which was introduced into strain ΔaveT to obtain the complemented strain CaveT. For overexpression of *aveT* in *S. avermitilis*, a 643-bp DNA fragment carrying the *aveT* ORF was amplified with primers LWS5 and LWS6. The PCR product was digested with HindIII/BamHI and inserted into pJL117 to generate pJL117-aveT. The 937-bp BglII fragment containing the *aveT* ORF and *ermE*p* from pJL117-aveT was then cloned into BamHI-digested pKC1139 to generate *aveT*-overexpressing vector pKC1139-ermp-aveT, in which *aveT* was controlled by the strong constitutive promoter *ermE*p*. pKC1139-ermp-aveT was introduced into ATCC 31267 and A-178 to obtain *aveT*-overexpressing strains OaveT and OaveT/A-178, respectively.

To construct an *aveM* (*sav_7490*) deletion mutant, a 457-bp 5′ flanking region (positions −335 to +122 relative to the *aveM* start codon) and a 437-bp 3′ flanking region (positions +1278 to +1714) were amplified with primer pairs LWS33/LWS34 and LWS35/LWS36, respectively. The two PCR fragments were digested with EcoRI/XbaI and XbaI/HindIII and simultaneously ligated into EcoRI/HindIII-digested pKC1139 to generate *aveM* deletion vector pΔaveM, which was transformed into ATCC 31267. The deletion in the resulting mutant with the *aveM* deletion, mutant ΔaveM, was confirmed by PCR using LWS37, LWS38, LWS39, and LWS40 as primers (see Fig. S1 in the supplemental material). When using primers LWS37 and LWS38, whose sequences flank the exchange regions, a 1.2-kb band appeared, whereas a 2.4-kb band was detected from ATCC 31267. When using primers LWS39 and LWS40, whose sequences are located within the deletion region of *aveM*, only ATCC 31267 produced a 301-bp band, as predicted (data not shown). To delete *aveM* in A-178, the pΔaveM vector was transformed into A-178 protoplasts. The expected mutant, termed ΔaveM/A-178, was isolated using the strategy used for selection of the ΔaveM mutant, and the deletion was confirmed by PCR using the same primers.

For complementation of strain ΔaveM, a 2.0-kb DNA fragment carrying the *aveM* ORF and its promoter was amplified with primers LWS41 and LWS42 and inserted into pSET152 to generate *aveM* gene-complemented vector pSET152-aveM, which was then introduced into strain ΔaveM to obtain the complemented strain CaveM. For overexpression of *aveM* in ATCC 31267, a 1.5-kb DNA fragment carrying the *aveM* ORF was amplified with primers LWS43 and LWS44 and cloned into pJL117 to

generate pJL117-aveM, in which *aveM* was controlled by *ermE*p*. pJL117-aveM was cut with EcoRI/HindIII, and the resulting 1.8-kb fragment containing the *aveM* ORF and *ermE*p* was inserted into pKC1139 to generate pKC1139-ermp-aveM, which was then introduced into ATCC 31267 to obtain *aveM*-overexpressing strain OaveM.

To construct an *aveT aveM* double deletion mutant, the pΔaveM vector was transformed into ΔaveT protoplasts. The expected mutant, ΔaveTaveM, was isolated by selection of the ΔaveM mutant.

To construct a *pepD2* (*sav_3620*)-overexpressing strain, a 3.3-kb DNA fragment carrying the *pepD2* ORF was amplified with primers LWS52 and LWS53 and ligated into pJL117 to generate pJL117-pepD2. The 3.6-kb EcoRI/HindIII fragment containing the *pepD2* ORF and *ermE*p* from pJL117-pepD2 was inserted into pKC1139 to generate pKC1139-ermp-pepD2, which was introduced into ATCC 31267 to obtain *pepD2*-overexpressing strain OpepD2.

To construct an *aco* (*sav_3706*, homologous to *sco3247*) deletion mutant, a 536-bp 5′ flanking region (positions −524 to +12 relative to the *aco* start codon) was amplified with primers GJ189 and GJ190, and a 613-bp 3′ flanking region (positions +1988 to +2600) was amplified with primers GJ191 and GJ192. The two PCR fragments were ligated into pKC1139 to generate an *aco* deletion vector, pΔaco, which was transformed into ATCC 31267 protoplasts. The deletions in the resulting mutants with a putative *aco* deletion were confirmed by PCR using GJ207, GJ208, aco-S, and aco-AS as primers. When primers GJ207 and GJ208, whose sequences flank the exchange regions, were used, a 1.3-kb band appeared, whereas a 3.3-kb band was detected from ATCC 31267. When primers aco-S and aco-AS, whose sequences are located within the deletion region of *aco*, were used, only ATCC 31267 produced a 320-bp band, as predicted (data not shown). The obtained *aco* deletion mutant was termed strain Δaco. All the primers used in this work are listed in Table 2.

Overexpression and purification of His_6-AveT. The *aveT* coding region of 196 amino acids was obtained by PCR using primers LWS48 and LWS49. The PCR fragment was cut with NdeI/BamHI and cloned into pET-28a(+) to generate expression plasmid pET28-aveT, whose sequence was confirmed by DNA sequencing and then transformed into *E. coli* BL21(DE3) for overexpression of His_6-AveT. Following induction by 0.4 mM IPTG (isopropyl-β-D-thiogalactopyranoside), the recombinant His_6-AveT protein was purified by Ni-nitrilotriacetic acid agarose chromatography (Qiagen, Germany) according to the manufacturer's protocol. The purified protein was stored at −80°C and used for electrophoretic mobility shift assays (EMSAs) and DNase I footprinting assays.

Determination of TSSs using 5′ RACE. A 5′/3′ rapid amplification of cDNA ends (RACE) kit (2nd generation; Roche, USA) was used to conduct 5′ RACE experiments to map the transcriptional start sites (TSSs) of *aveT*, *pepD2*, and *aveM*. Total RNA (4 μg) extracted from a 144-h culture of ATCC 31267 grown in fermentation medium FM-I was used for cDNA synthesis with 40 pmol of gene-specific primer aveTSP1, pepD2SP1, or aveMSP1. The synthesized cDNAs were purified using an agarose gel DNA recovery kit (Bioteke Corporation, Beijing, China) and treated with terminal deoxynucleotidyltransferase for 30 min to add an oligo(dA) tail to the 3′ end. The tailed cDNA was amplified by PCR using the oligo(dT) anchor primer and a second inner gene-specific primer, aveTSP2, pepD2SP2, or aveMSP2. A single specific band was obtained for *aveT*. To obtain a single specific band for *pepD2* and *aveM*, the original PCR product (diluted 100-fold) was amplified in a second PCR with an anchor primer and a nested primer, pepD2SP3 or aveMSP3. The final PCR products were purified with the DNA recovery kit for sequencing. The first nucleotide next to the oligo(dA) sequence was mapped as the TSS.

EMSA. A DIG gel shift kit (2nd generation; Roche) was used as described previously (28). In brief, DNA probes were amplified by PCR using the primers listed in Table 2, labeled with digoxigenin (DIG) at the 3′ ends, and incubated with various quantities of His_6-AveT at 25°C for 30 min in a binding buffer (vial 5) containing 1 μg poly[d(I·C)] (vial 9) in a total volume of 20 μl. Following incubation, the binding reactions were separated by electrophoresis (with 5% native polyacrylamide gels and 0.5× TBE [Tris-borate-EDTA] as the running buffer) and the DNAs were transferred onto a positively charged nylon membrane by electroblotting. The membranes were dried and exposed to UV radiation to cross-link the DNA fragments. Protein-bound and free DNAs were detected by chemiluminescence, and the signals were recorded on X-ray film (Fuji, Japan).

DNase I footprinting assay. A nonradiochemical capillary electrophoresis method was used for DNase I footprinting (36). To characterize the binding site of the AveT protein in the *aveT-pepD2* intergenic region, a 395-bp 6-carboxyfluorescein (FAM) fluorescence-labeled DNA fragment covering the entire intergenic region was prepared by PCR using primer pair FAM-LWS15/LWS16 (Table 2). Following purification from the agarose gel, 400 ng of the labeled DNA fragment and various concentrations of His_6-tagged AveT protein were incubated at 25°C for 30 min in a 25-μl reaction volume. DNase I (0.016 units) digestion was carried out for 40 s at 37°C and stopped with 60 mM EDTA. After extraction in phenol-chloroform and precipitation in ethanol, samples were subjected to capillary electrophoresis and electropherograms were analyzed as described previously (28).

Real-time RT-PCR analysis. Total RNA was isolated, using the TRIzol reagent (Tiangen, China), from cultures of *S. avermitilis* grown in FM-I for various times. The quality and quantity of the RNAs were examined using a NanoVue Plus spectrophotometer (GE Healthcare, United Kingdom) and confirmed by electrophoresis. The transcription levels of various genes were determined by real-time reverse transcription-PCR (RT-PCR) analysis as described previously (28) using the primers listed in Table 2. The *hrdB* (*sav_2444*) gene was used as an internal control to normalize the levels of transcription of the samples. A DNase I-treated RNA sample that did not undergo reverse transcription was used as a negative control to rule out chromosomal DNA contamination.

Fermentation and HPLC analysis of avermectins. Fermentation of the *S. avermitilis* strains and high-pressure liquid chromatography (HPLC) analysis of avermectin production in the fermentation culture were performed as described previously (34).

Preparation of *S. avermitilis* fermentation supernatant for EMSAs. *S. avermitilis* fermentation cultures grown in FM-I for 10 days were centrifuged at 4,000 × *g* for 10 min. Two milliliters of supernatant was dried by vacuum freezing, dissolved in 200 μl distilled water, and subjected to EMSAs.

RESULTS

AveT is a positive regulator of morphological differentiation and avermectin production. According to the *S. avermitilis* genome database (http://avermitilis.ls.kitasato-u.ac.jp), the *aveT* (*sav_3619*) gene contains 591 nucleotides (nt) and encodes a putative TFR (predicted molecular mass, 21.8 kDa) whose function is unknown. The convergently transcribed gene *sav_3618* is located downstream of *aveT* and encodes a putative transmembrane transport protein. The divergently transcribed gene *pepD2* (*sav_3620*) is located upstream of *aveT* and encodes a putative tricorn core peptidase (Fig. 1A). BLAST analysis revealed that AveT homologs are widely distributed among *Streptomyces* species and display high amino acid sequence identities (75 to 78%) (see Fig. S2 in the supplemental material), suggesting that this TFR has important biological functions in *Streptomyces*.

To clarify the function of AveT in *S. avermitilis*, we constructed *aveT* deletion mutant ΔaveT (Fig. 1B) and *aveT*-overexpressing strain OaveT. OaveT grew normally on the solid media YMS and MM, whereas mutant ΔaveT displayed obvious delays of aerial hypha formation and sporulation on these media (Fig. 2A). HPLC analysis of the fermentation products was performed after culture in FM-I for 10 days. Avermectin production in mutant ΔaveT was ~50% lower than that in WT strain ATCC 31267 (Fig. 2B). To determine whether this change was due solely to the *aveT*

TABLE 2 Primers used in this study

Primer purpose and primer	DNA sequence[a] (5′–3′)	Use
Gene disruption, complementation, and overexpression		
LWS1	CGGGATCCCCAGCGCCTTGACGGTCT (BamHI)	Deletion of *aveT* gene
LWS2	GTACTCGGCGGTGCTCGACTGCCTCCCACGCAGGAAT	Deletion of *aveT* gene
LWS3	ATTCCTGCGTGGGAGGCAGTCGAGCACCGCCGAGTAC	Deletion of *aveT* gene
LWS4	CCCAAGCTTTCGCTGTGCCCCTCCTTG (HindIII)	Deletion of *aveT* gene
LWS5	CCCAAGCTTGGAGGGAGGGGAGAGAGGG (HindIII)	Overexpression of *aveT* in *S. avermitilis*
LWS6	CGGGATCCCGAAGCAGGAGAGGCGAGTG (BamHI)	Overexpression of *aveT* in *S. avermitilis*
LWS7	GCGAGTGCGTCTTGAAGG	Confirmation of *aveT* deletion in ΔaveT
LWS8	CGGTGAGCAGCAGGGTCT	Confirmation of *aveT* deletion in ΔaveT
LWS9	CTACGACGCCCTGACCAT	Confirmation of *aveT* deletion in ΔaveT
LWS10	GCATCTCGTTCGTCTCGG	Confirmation of *aveT* deletion in ΔaveT
LWS11	CGGGATCCTCGGACTCGGGGTTCACCT (BamHI)	Complementation of ΔaveT
LWS12	GCTCTAGAGAGGGCGTACTCCCGGTC (XbaI)	Complementation of ΔaveT
LWS33	GGAATTCCGCTGAACGTGATCGTGCC (EcoRI)	Deletion of *aveM* gene
LWS34	GCTCTAGAAGGACGACCATCAACTGGG (XbaI)	Deletion of *aveM* gene
LWS35	GCTCTAGATACGGCGCTGCTGAACAC (XbaI)	Deletion of *aveM* gene
LWS36	CCCAAGCTTCGGAACCTCGCCTACGAC (HindIII)	Deletion of *aveM* gene
LWS37	AGGCAGACCTCCCATCCG	Confirmation of *aveM* deletion in ΔaveM
LWS38	TGCTCGACCTGCGCCTGA	Confirmation of *aveM* deletion in ΔaveM
LWS39	TTGTCGCTGAGCAACCAC	Confirmation of *aveM* deletion in ΔaveM
LWS40	GGAATACACCGAACATGCC	Confirmation of *aveM* deletion in ΔaveM
LWS41	GGAATTCAGGCAGACCTCCCATCCG (EcoRI)	Complementation of ΔaveM
LWS42	GCTCTAGAGCGCTCACATGTGGACGA (XbaI)	Complementation of ΔaveM
LWS43	GCTCTAGAGGCTTCCCTGGAGTGGTT (XbaI)	Overexpression of *aveM* in *S. avermitilis*
LWS44	CCCAAGCTTGCGCTCACATGTGGACGA (HindIII)	Overexpression of *aveM* in *S. avermitilis*
LWS52	GCTCTAGAGCGGAAAAGCATGGGTTAG (XbaI)	Overexpression of *pepD2* in *S. avermitilis*
LWS53	CCCAAGCTTTCTGCCTTGTTCATCGTCT (HindIII)	Overexpression of *pepD2* in *S. avermitilis*
LWS48	GGAATTCCATATGACTGAGACCGCAACGGTGCG (NdeI)	Overexpression of His_6-tagged AveT protein in *E. coli*
LWS49	CGGGATCCTCAGGCGCCGAGGGCGGG (BamHI)	Overexpression of His_6-tagged AveT protein in *E. coli*
GJ189	CGGAATTCTATCCCACCTCGTCGAACAC (EcoRI)	Deletion of *aco* gene
GJ190	GAAGATCTCGTAGCGATCATCGAGCTTC (BglII)	Deletion of *aco* gene
GJ191	GAAGATCTAGGAATGGCCACTGGTCTC (BglII)	Deletion of *aco* gene
GJ192	CCCAAGCTTGTTGCTCGCATGAGGTTCTT (HindIII)	Deletion of *aco* gene
GJ207	TCGACGTGAAGTGGAAGTAGAG	Confirmation of *aco* deletion in Δaco
GJ208	AGATGCAGGAACGCAGTACG	Confirmation of *aco* deletion in Δaco
aco-S	GCGAGCATCCACTACAACCT	Confirmation of *aco* deletion in Δaco
aco-AS	GGGGTCAGGAAGAGGAAGAC	Confirmation of *aco* deletion in Δaco
5′ RACE		
Oligo(dT) anchor primer	GACCACGCGTATCGATGTCGACTTTTTTTTTTTTTTTV	
Anchor primer	GACCACGCGTATCGATGTCGAC	
aveTSP1	GCATCTCGTTCGTCTCGG	Identification of TSS of *aveT*
aveTSP2	CTCGCAGTTGTTCTCCCG	Identification of TSS of *aveT*
pepD2SP1	GGTGAAGTAGGAGAAGGGCT	Identification of TSS of *pepD2*
pepD2SP2	TGCTGCCCCAGTAGGTGAG	Identification of TSS of *pepD2*
pepD2SP3	CAGGTGGATCTCCGGGAC	Identification of TSS of *pepD2*
aveMSP1	CGTGTTCAGGAGCGAGAG	Identification of TSS of *aveM*
aveMSP2	CGGTGACCAGCATCTCGA	Identification of TSS of *aveM*
aveMSP3	AGAACCCGAGGTCCGCCT	Identification of TSS of *aveM*
EMSA		
LWS13	TCGGACTCGGGGTTCACCT	Probe *aveT_pepD2*_int
LWS14	CTCGGGCGTGATCCGACT	Probe *aveT_pepD2*_int
LWS19	GTGACCCACGACACGTACGAAACGGTTTCGTTTCGCTCGCTCT	Probe 1
LWS20	AGAGCGAGCGAAACGAAACCGTTTCGTACGTGTCGTGGGTCAC	Probe 1
LWS21	GTGACCCACGACACGTAAAGCTTGGTTTGGAATTCCTCGCTCT	Probe 1m
LWS22	AGAGCGAGGAATTCCAAACCAAGCTTTACGTGTCGTGGGTCAC	Probe 1m
LWS23	TGGTGCCTCGGTCCTTGG	Probe *aveM_sav_7491*_int
LWS24	CGGGTGCTTTCGGTCAGA	Probe *aveM_sav_7491*_int
LWS50	ACGCCTGGTCCTCCGA	Probe *aveRp*

(Continued on following page)

TABLE 2 (Continued)

Primer purpose and primer	DNA sequence[a] (5′–3′)	Use
LWS51	TGAGTTCTTCTGGTTTCCGAG	Probe *aveRp*
LWS58	ATGGTCGGGAACCTCCGCAA	Probe *aveA1p*
LWS59	CTGTGTCCTCACCGCTAGGC	Probe *aveA1p*
DNase I footprinting assay		
FAM-LWS15	CCAGCCACAGGTCGTCCT	*aveT-pepD2* intergenic region
LWS16	TGGTCAGGGCGTCGTAGC	*aveT-pepD2* intergenic region
Real-time RT-PCR		
LWS25	CCGTGTCGTTCGAAGCA	*aveT* ORF
LWS26	GAGTACAGCTCGGCCTC	*aveT* ORF
LWS27	CAAGGCGAAGAAGTCCGAAC	*pepD2* ORF
LWS28	CCGCAGATCTCCTTCGTCCA	*pepD2* ORF
LWS29	GCGACCGGCTATCTGTCC	*aveM* ORF
LWS30	GAAGAAGACCGCCGACCAC	*aveM* ORF
LWS31	ACGCTCACCAACGTCCT	*sav_7491* ORF
LWS32	CCCGCCTCGACGTAGCC	*sav_7491* ORF
LWS54	CAGAAGAACTCACGCTCGTC	*aveR* ORF
LWS55	ACTCTTTCCACAGCCCATTC	*aveR* ORF
LWS56	CGGACAGGACTACGCACTTC	*aveA1* ORF
LWS57	ACGAGATACGACCGGAGATG	*aveA1* ORF

[a] Underlining represents the sequence of the restriction endonuclease identified in parentheses at the end of the sequence.

deletion, we constructed *aveT*-complemented strain CaveT using pSET152-based vector pSET152-aveT, which contained the *aveT* coding region and its promoter. The avermectin yield was restored in CaveT. Overexpression of *aveT* (strain OaveT) increased the avermectin yield by ~1.2-fold. The avermectin contents of vector control strains WT/pSET152 and WT/pKC1139 were nearly the same as those of ATCC 31267 (Fig. 2B). To rule out the possibility that altered avermectin yields in strains ΔaveT and OaveT resulted from changes in cell growth, we examined the growth of strains ATCC 31267, ΔaveT, and OaveT in soluble fermentation medium FM-II. Deletion and overexpression of *aveT* had no effect on cell growth (Fig. 2C). Taken together, these findings indicate that AveT acts to positively regulate morphological differentiation and avermectin production.

AveT activates *aveR* but represses its own gene and adjacent gene *pepD2*. AveT has a positive effect on avermectin production. In fermentation medium FM-I, avermectin production in the WT strain was not observable by HPLC until day 2 and then increased gradually until the end of fermentation day 10 (data not shown). The transcription profile of *aveT* in ATCC 31267 grown in FM-I was analyzed by real-time RT-PCR. *aveT* transcription was detectable throughout the fermentation process (Fig. 3A). The level of *aveT* transcription increased starting on day 1, reached its maximal level on day 4, and then gradually declined and remained at a low level from day 6 onward, suggesting that AveT affects avermectin production mainly in the middle stage of fermentation.

To investigate the possibility that AveT regulates avermectin production through CSR AveR, which then activates avermectin biosynthesis, we performed real-time RT-PCR analysis using RNAs isolated from strains ATCC 31267, ΔaveT, and OaveT grown in FM-I for 2 days (early exponential phase, when avermectin biosynthesis was initiated) or 6 days (stationary phase). In comparison with the transcription levels in ATCC 31267, those of *aveR* and structural gene *aveA1* (which encodes polyketide synthase AVES1) were decreased in ΔaveT and increased in OaveT on both days (Fig. 3B), consistent with the avermectin yield data for these strains. These findings suggest that AveT affects avermectin production by stimulating the transcription of cluster-situated activator gene *aveR*.

Based on the model TetR/TetA regulatory paradigm (19), we predicted that AveT regulates the expression of its own gene and adjacent divergently transcribed gene *pepD2*. The transcription levels of *aveT* and *pepD2* were examined using the same RNA samples (Fig. 3B). The *aveT* transcription level was higher in OaveT than in ATCC 31267, confirming the overexpression of *aveT* in OaveT. The *pepD2* transcription level was very low in ATCC 31267 and slightly decreased in OaveT, whereas the expression of *aveT* and *pepD2* was strikingly upregulated in ΔaveT. These findings indicate that AveT functions as a repressor of its own gene and *pepD2*.

AveT binds specifically to the bidirectional *aveT-pepD2* promoter region. To determine whether AveT directly regulates the genes mentioned in the preceding section, we performed *in vitro* EMSAs. Soluble full-length recombinant His_6-tagged AveT protein was overexpressed in *E. coli*, and purified His_6-AveT was used for EMSAs. The promoter regions of *aveR* and *aveA1* were labeled as probes *aveRp* and *aveA1p*, respectively. The probe *aveT_pepD2*_int was designed to cover the entire *aveT-pepD2* intergenic region, which contains two divergent promoters (Fig. 4A). His_6-AveT did not bind to probe *aveRp* or *aveA1p*, even at a high protein concentration (2.8 μM) (Fig. 4B), indicating that the positive regulatory effect of AveT on avermectin production is indirect. The probe *aveT_pepD2*_int gave a clearly retarded signal. Binding specificity was evaluated by addition of excess unlabeled specific probe *aveT_pepD2*_int (lane S), which competed strongly with labeled probe *aveT_pepD2*_int for binding to AveT, and of excess unlabeled nonspecific competitor DNA (lane N), which did not reduce or abolish the delayed signal. A nonspecific *hrdB* probe was labeled and used as a negative control (Fig. 4B). These findings indicate that AveT directly regulates the transcription of its own

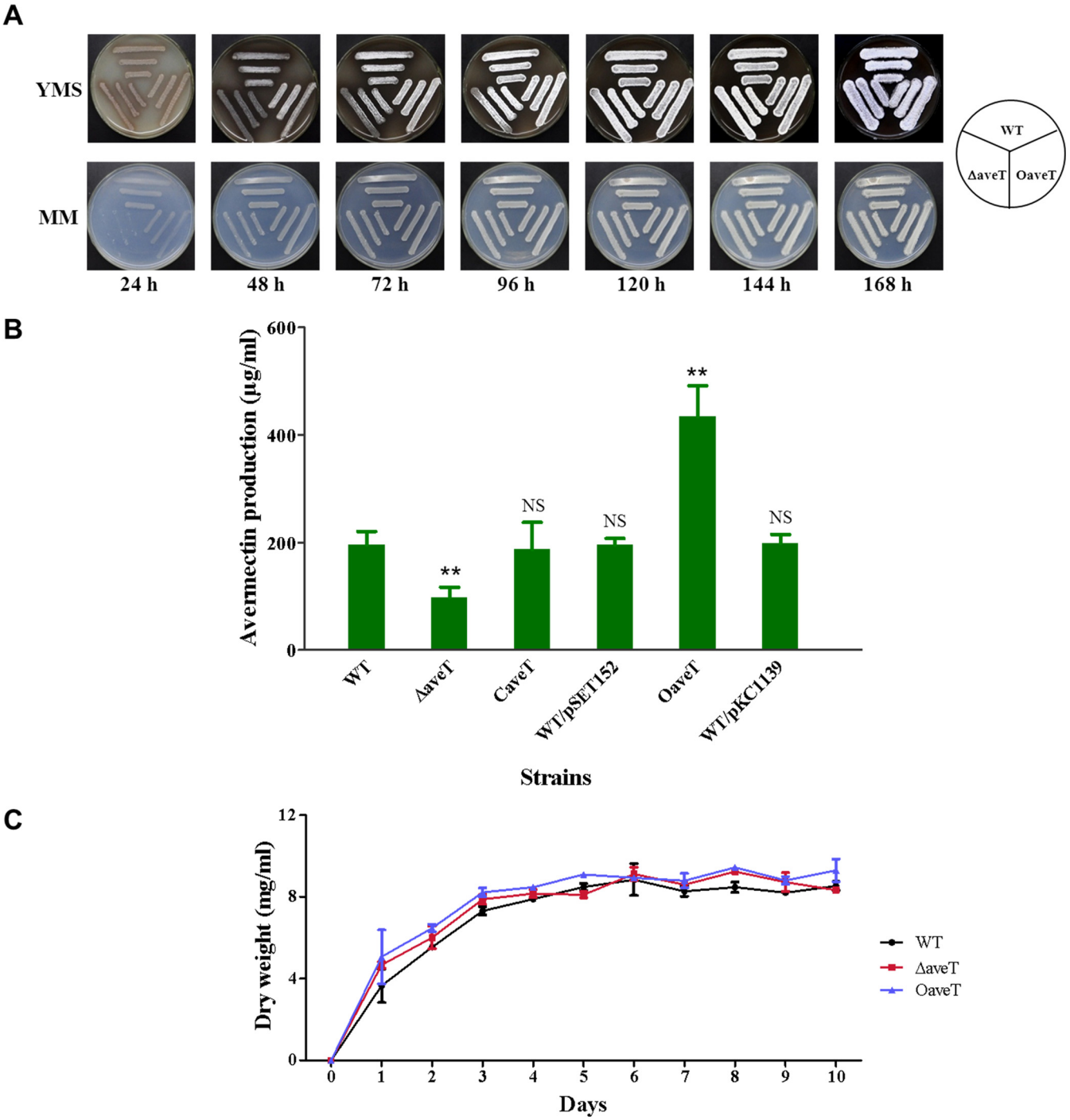

FIG 2 Effects of deletion and overexpression of *aveT* on morphological development (A), avermectin production (B), and growth (C) in *S. avermitilis*. (A) WT strain ATCC 31267, *aveT* deletion mutant ΔaveT, and *aveT*-overexpressing strain OaveT were grown on YMS or MM plates at 28°C and photographed every 24 h. (B) Comparative avermectin production in *aveT* mutant strains. The WT, ΔaveT, and OaveT strains are as described in the legend to panel A, CaveT is an *aveT*-complemented strain of ΔaveT, WT/pSET152 is the WT strain carrying control integration plasmid pSET152, and WT/pKC1139 is the WT carrying control multiple-copy plasmid pKC1139. Strains were cultured in FM-I medium for 10 days. Error bars, standard deviations from three replicate flasks. **, $P < 0.01$ for comparison of means for mutant versus WT strains; NS, not significant. (C) Growth curves of the WT, ΔaveT, and OaveT strains in FM-II medium.

gene and adjacent gene *pepD2* through binding to their promoter regions.

Identification of the AveT-binding site in the *aveT-pepD2* intergenic region. To elucidate the mechanism whereby AveT regulates *aveT* and *pepD2*, we determined the precise binding site of AveT in the *aveT-pepD2* intergenic region and the promoter structures of the two genes. To determine the AveT-binding sequence, we performed DNase I footprinting experiments using a

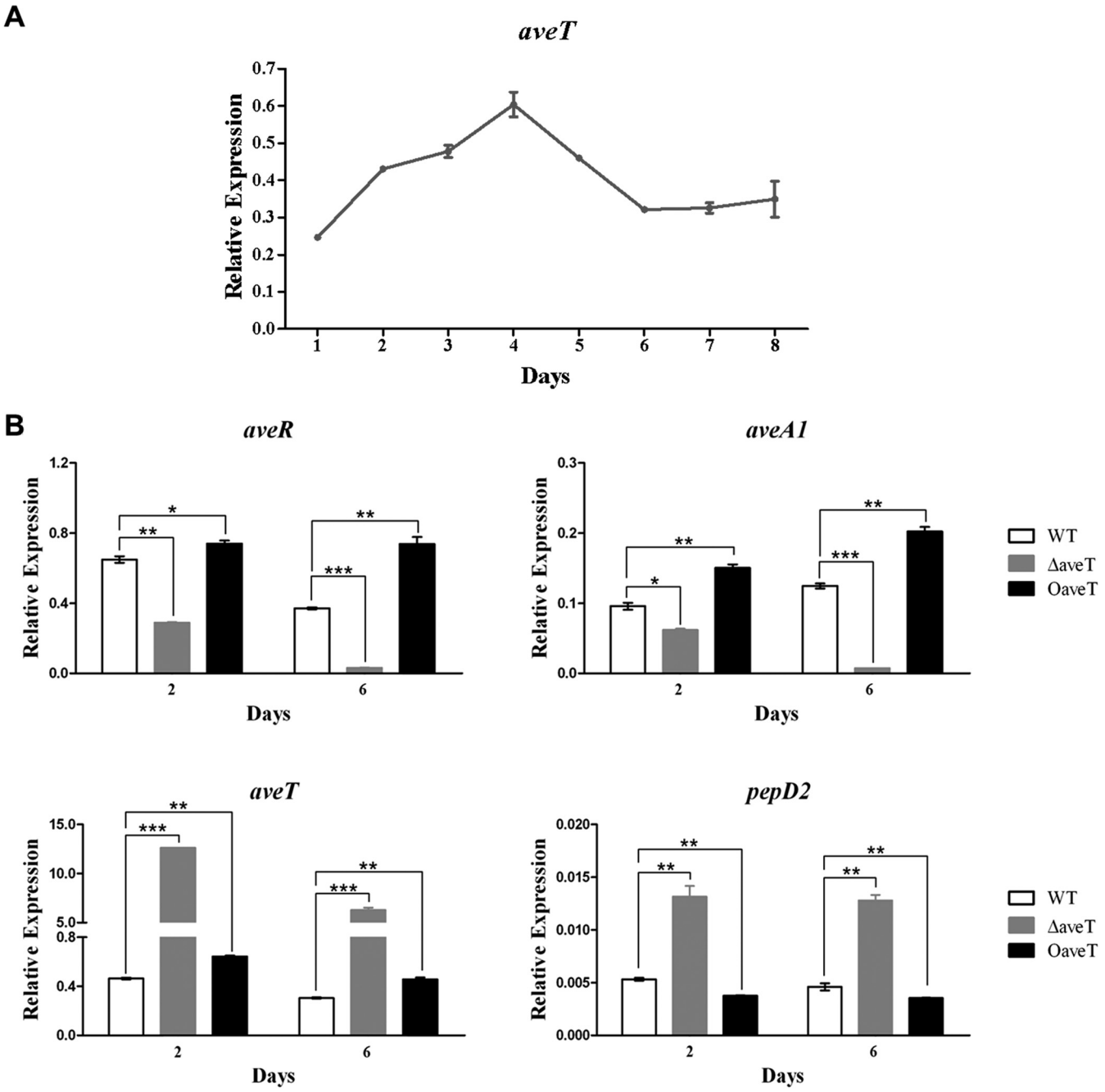

FIG 3 Transcriptional analysis of *aveT* and related genes by real-time RT-PCR. (A) Transcription profile of *aveT* during the avermectin production process in WT strain ATCC 31267. (B) *aveR*, *aveA1*, *aveT*, and *pepD2* transcription levels in the WT, ΔaveT, and OaveT strains. RNA samples were isolated from 2- and 6-day fermentation cultures in FM-I. Relative transcription levels were obtained after normalization against the level of transcription of the internal reference gene *hrdB* at specific time points. *aveT*, 97-bp transcript amplified from the remaining *aveT* ORF in ΔaveT with primers LWS25 and LWS26; error bars, standard deviations from three independent experiments. *P* values were determined by Student's *t* test. *, $P < 0.05$; **, $P < 0.01$; ***, $P < 0.001$.

395-bp FAM-labeled DNA probe that comprised the *aveT-pepD2* intergenic region in the presence and absence of the His_6-AveT protein. A protected 35-nt stretch was found on the coding strand of *aveT* (Fig. 5A). The TSSs of the genes were determined by 5′ RACE PCR analysis. The *aveT* TSS was mapped to a G residue at position 72 nt upstream of the translational start codon of *aveT*, and the *pepD2* TSS was mapped to a G residue at position 1 nt upstream of the translational start codon of *pepD2* (Fig. 5B; see also Fig. S3 in the supplemental material). Determination of these TSSs led to the putative −10 and −35 promoter sequences indicated by boxes in Fig. 5B. *aveT* and *pepD2* represent two known initiation mechanisms in prokaryotes. The initiation of *aveT* translation is a Shine-Dalgarno (SD) initiation mechanism. SD initiation has long been regarded as the predominant mechanism in prokaryotes. The second mechanism, termed "leaderless initiation," is epitomized by translation initiation of *pepD2*, in which the mRNA lacks a 5′ untranslated region

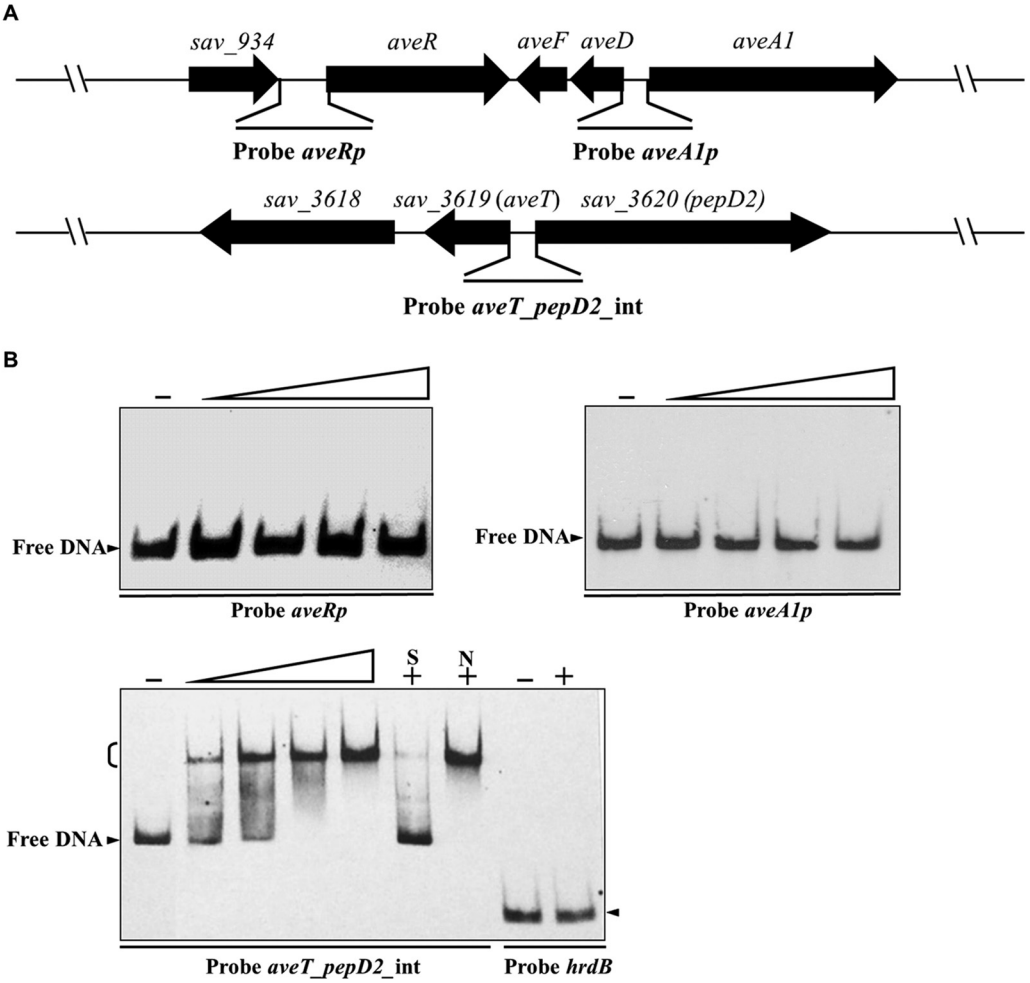

FIG 4 EMSAs of AveT binding to the *aveT-pepD2* intergenic region. (A) Schematic representation of the probes used for EMSAs. Probe *aveRp*, 527-bp DNA fragment from positions +49 to −478 relative to the start codon of *aveR*; probe *aveA1p*, 333-bp DNA fragment from positions −6 to −338 relative to the start codon of *aveA1*; probe *aveT_pepD2*_int, a 248-bp DNA fragment covering the *aveT-pepD2* intergenic region. Probes *aveRp* and *aveA1p* cover the putative TSSs of *aveR* and *aveA1*, respectively. (B) EMSAs of the interaction of probes *aveRp*, *aveA1p*, and *aveT_pepD2*_int with purified His_6-AveT protein. Each reaction mixture contained 0.15 nM labeled probe. EMSAs with 300-fold unlabeled specific probe (lane S) or nonspecific competitor DNA (lane N) were performed to confirm the specificity of the band shifts. Labeled probe *hrdB* was used as a negative control. Labeled probes were incubated in the absence (lanes −) or presence of various amounts of His_6-AveT. The concentrations of the His_6-AveT protein for the probes were as follows: for *aveRp* and *aveA1p*, 0.4, 1.2, 2.0, and 2.8 μM; for *aveT_pepD2*_int, 0.005, 0.01, 0.05, and 0.1 μM; for *hrdB*, 2.8 μM. Competition experiments were performed using 0.1 μM His_6-AveT. Arrowheads, free probe; bracket, AveT-DNA complex.

(UTR) and therefore has no SD sequence. Leaderless initiation has been observed in many species of bacteria and archaea (37, 38). The binding sequence of AveT extends from positions −58 to −24 nt relative to the *aveT* TSS and from positions −90 to −56 nt relative to the *pepD2* TSS (Fig. 5B). The protected region overlaps the potential −35 region of the *aveT* promoter and is located upstream but close to the potential −35 region of the *pepD2* promoter, suggesting that AveT directly represses expression of its own gene and *pepD2*, most likely by impeding the access of RNA polymerase to the respective promoter regions.

Most TFRs form symmetric dimers and bind to palindromic sequences (19). DNAMAN analysis of the AveT-binding region revealed an 18-bp palindromic sequence CGAAACGGTTTCGTTTCG, where the underlining indicates inverted repeats (Fig. 5A and B), which may function as the target site of AveT binding. To assess the importance of the palindromic sequence in AveT binding, it was mutated, as shown in Fig. 5C. The binding activity of AveT with probes that contained either the intact 18-bp palindromic sequence or the mutated sequence was determined by EMSAs. The affinity of AveT for mutated probe 1m, which lacked inverted repeats, was abolished completely, and a strongly retarded signal was observed between AveT and corresponding WT probe 1 (Fig. 5D). These findings indicate that the 18-bp palindromic sequence is essential for AveT binding.

Prediction and verification of new AveT target genes. Transcriptional regulators typically recognize similar DNA motifs in the promoter regions of different target genes. EMSAs and footprinting assays revealed an 18-bp palindromic sequence that plays an important role in AveT binding. The similar palindromic sequences were found in the promoter regions of *aveT* homologs, including *sco3167*, *sgr_4317*, *scab53291*, *sven_3001*, *sclav_2302*, *sli_3521*, and *strs4_04951*. Analysis of these palindromic se-

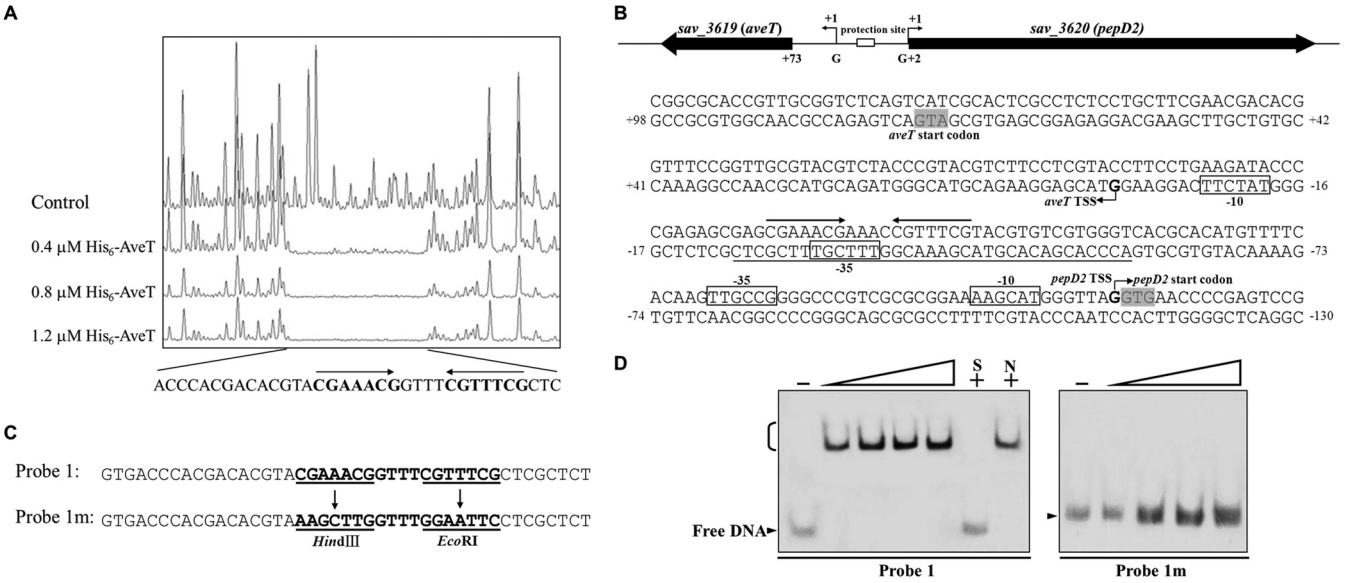

FIG 5 Determination of AveT-binding site. (A) DNase I footprinting assay of AveT in the *aveT-pepD2* intergenic region. Upper fluorogram, control reaction without protein. Protection patterns were obtained with increasing concentrations (0.4, 0.8, 1.2 μM) of the His_6-AveT protein. (B) Nucleotide sequences of the *aveT-pepD2* promoter region and AveT-binding site. Numbers, distances (in nucleotides) from the TSS of *aveT*; solid line, AveT-binding site; straight arrows, inverted repeats; bent arrows, TSSs; boxes, putative −10 and −35 regions; shaded areas, translational start codons. (C) Mutations introduced into the 18-bp palindromic sequence. Each probe was 43 bp. Probe 1 was WT DNA containing an intact 18-bp palindromic sequence. Inverted repeats in probe 1 were replaced with HindIII and EcoRI sites to produce mutated probe 1m. Underlining, altered nucleotides. (D) EMSAs using probe 1 and mutated probe 1m. Each reaction mixture contained 0.75 nM labeled probe. The concentrations of the His_6-AveT protein for the probes were as follows: for probe 1, 0.1, 0.2, 0.3, and 0.4 μM; for probe 1m, 0.4, 0.8, 1.2, and 1.6 μM.

quences using the WebLogo program (http://weblogo.berkeley.edu/) revealed a consensus sequence, CGAAACSRTTTMGT TYHS (where S is C or G; R is G or A; M is C or A; Y is T or C; and H is A, C, or T) (see Fig. S4 in the supplemental material). We used this consensus motif to scan the *S. avermitilis* genome in a search for new putative target genes of AveT. The detected putative AveT target sites are listed in Table S1 in the supplemental material. Among them, 13 putative targets were selected according to two criteria as follows and confirmed experimentally by EMSA: (i) candidate AveT-binding sites have relatively high degrees of similarity to the conserved sequence, and (ii) the putative target genes are well annotated. The bidirectional *aveM* (*sav_7490*)-*sav_7491* promoter region was found to contain inverted repeats identical to those in the identified AveT-binding site. *aveM* encodes a putative transmembrane efflux protein that belongs to the major facilitator superfamily (MFS), and *sav_7491* encodes a hypothetical protein (Fig. 6A). AveT interacted specifically with the *aveM-sav_7491* intergenic region (Fig. 6B). The specificity of the AveT-DNA interaction was tested by competition assay with an excess of unlabeled specific and nonspecific DNA competitors. AveT did not interact with the bidirectional promoter regions of *tagG* (*sav_5081*, encoding a putative ABC transporter permease protein)-*sav_5082* (encoding a putative TFR), *sav_2282* (encoding a putative acyl carrier protein)-*sav_2283* (encoding a putative aldehyde dehydrogenase), *lplA* (*sav_2577*, encoding a putative multiple-sugar ABC transporter substrate-binding protein)-*sav_2578* (encoding a putative sugar hydrolase), and *sav_7270* (encoding a putative LacI-family transcriptional regulator)-*sav_7271* (encoding a putative multiple-sugar ABC transporter substrate-binding protein) or the promoter regions of *ectA* (*sav_6398*, encoding an L-2,4-diaminobutyrate acetyltransferase), *pabC2* (*sav_6852*, encoding a putative aminodeoxychorismate lyase), *sav_7048* (encoding a putative cation efflux system protein), *nrdL* (*sav_3026*, encoding a putative ribonucleoside diphosphate reductase alpha chain), *pmmB* (*sav_3343*, encoding a putative phosphomannomutase), *sav_3560* (encoding a putative two-component system sensor kinase), *sav_4488* (encoding a putative simple sugar ABC transporter substrate-binding protein), and *pfkA3* (*sav_7123*, encoding a 6-phosphofructokinase) (data not shown).

To evaluate the effect of AveT on the expression of newly identified target genes *aveM* and *sav_7491*, we performed real-time RT-PCR analysis. The *aveM* and *sav_7491* transcription levels were markedly increased in strain ΔaveT and decreased in strain OaveT relative to the levels in strain ATCC 31267 at both day 2 and day 6 (Fig. 6C), indicating that AveT represses the expression of *aveM* and *sav_7491*. The *aveM* transcription level was increased >240-fold in ΔaveT in comparison with that in ATCC 31267, suggesting that *aveM* is the primary target of AveT. The TSS of *aveM* was determined, and the AveT-binding site overlaps the potential −35 region of the *aveM* promoter (see Fig. S5 in the supplemental material), indicating that the regulation mechanism of AveT on its own gene (*aveT*) and *aveM* is similar.

The relationship of *pepD2* and *aveM* with avermectin production. Because *pepD2* and *aveM* were identified to be the target genes of AveT, we further investigated their roles in avermectin production. The relationship of *sav_7491* (another AveT target gene that encodes an unknown protein) with avermectin production was not investigated. Overexpression of *pepD2* in ATCC 31267 had no significant effect on avermectin production (Fig. 7A), suggesting that this gene is not involved in avermectin biosynthesis.

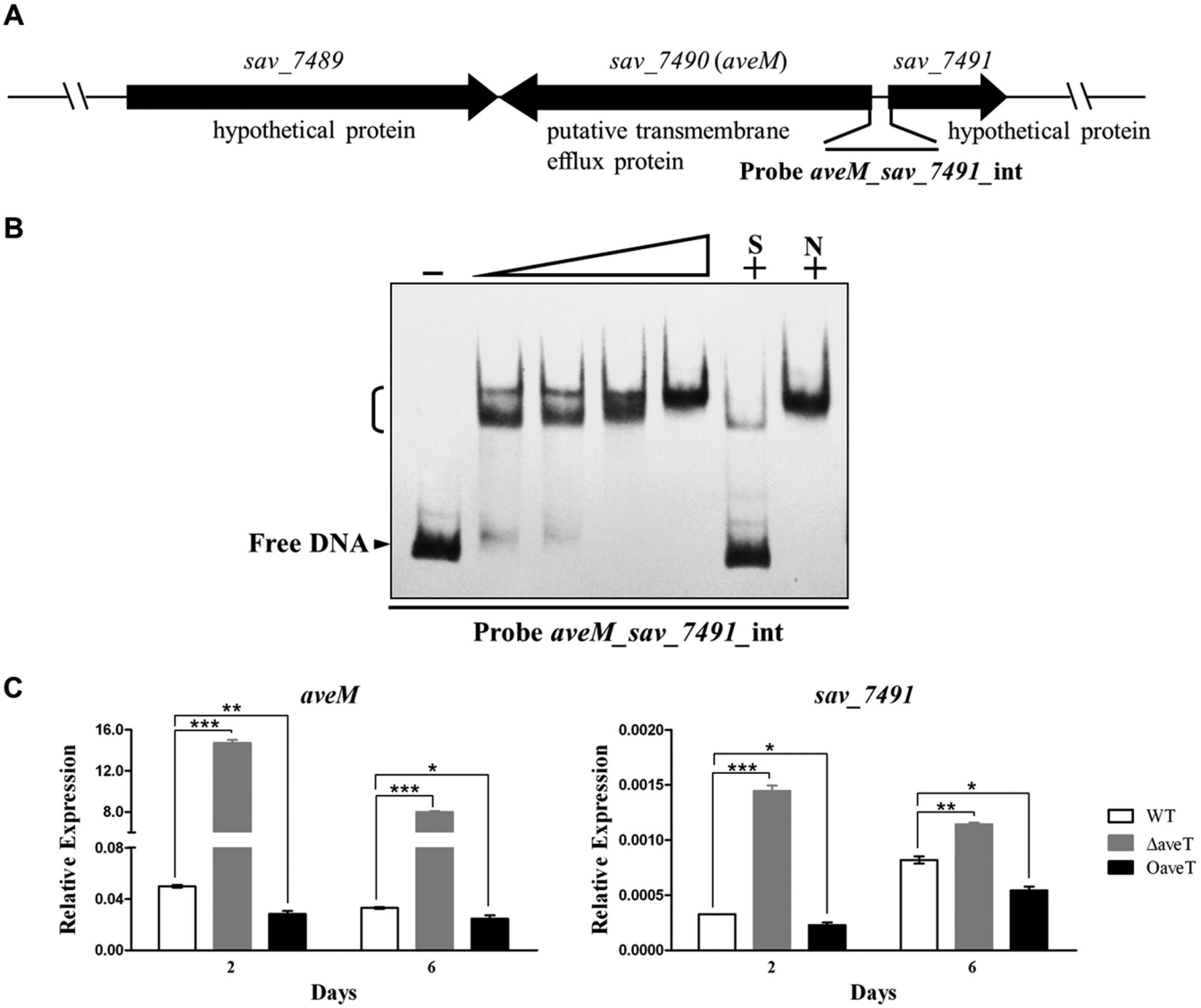

FIG 6 EMSAs of AveT binding to the *aveM-sav_7491* intergenic region and transcriptional analysis of *aveM* and *sav_7491* by real-time RT-PCR. (A) Schematic representation of probe *aveM_sav_7491*_int (a 178-bp DNA fragment covering the *aveM-sav_7491* intergenic region), used for EMSAs. (B) EMSAs of the interaction of probe *aveM_sav_7491*_int with purified His_6-AveT protein. Each lane contained 0.15 nM labeled probe. The concentrations of His_6-AveT for probe *aveM_sav_7491*_int were 0.005, 0.01, 0.05, and 0.1 μM. (C) *aveM* and *sav_7491* transcription levels in the WT, ΔaveT, and OaveT strains. *P* values were determined by Student's *t* test. *, $P < 0.05$; **, $P < 0.01$; ***, $P < 0.001$.

AveT positively regulates avermectin production, and *aveM* appears to be an important AveT target, suggesting a possible role of *aveM* in avermectin production. To test this possibility, we constructed *aveM* deletion mutant ΔaveM (see Fig. S1 in the supplemental material), *aveM*-overexpressing strain OaveM, and *aveM*-complemented strain CaveM. Comparisons of the levels of avermectin production among the various strains revealed that the *aveM* deletion (strain ΔaveM) led to a level of avermectin production ~3.5-fold higher than that in parental strain ATCC 31267, whereas upregulation of *aveM* expression (strain OaveM) led to an ~35% reduction of the avermectin yield (Fig. 7B). Avermectin production was restored to the WT level in the complemented strain CaveM, demonstrating that *aveM* deletion was the cause of increased avermectin production in strain ΔaveM. These findings indicate that *aveM* has a negative effect on avermectin production.

Interestingly, the expression level of *aveM* in ATCC 31267 was low (Fig. 6C). Deletion of *aveM* led to a striking increase in avermectin production, suggesting that this gene plays a crucial role in avermectin biosynthesis. Avermectin production in *aveT aveM* double deletion mutant ΔaveTaveM was much lower than that in strain ΔaveM (Fig. 7B), indicating that the altered avermectin production in strains ΔaveT and OaveT did not result simply from variable expression of *aveM*; i.e., other AveT targets may also affect avermectin production.

To assess the effect of *aveM* on morphological differentiation, phenotypic observations were performed. *aveM* deletion did not result in significant morphological changes. However, *aveM*-

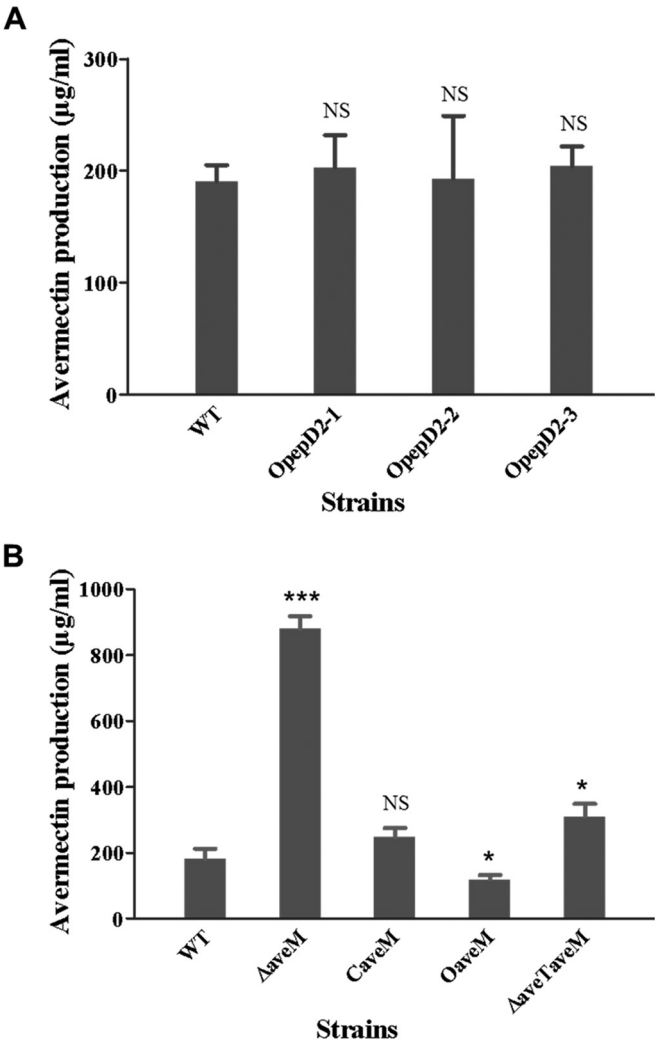

FIG 7 Role of *pepD2* and *aveM* in avermectin production. (A) Avermectin production in the WT and *pepD2*-overexpressing transformants OpepD2-1, OpepD2-2, and OpepD2-3. (B) Avermectin production in the WT and *aveM* mutant strains. ΔaveM, *aveM* deletion mutant; CaveM, *aveM*-complemented strain of ΔaveM; OaveM, *aveM*-overexpressing strain; ΔaveTaveM, *aveT aveM* double deletion mutant. All strains were cultured in FM-I for 10 days. *P* values were determined by Student's *t* test. *, $P < 0.05$; ***, $P < 0.001$; NS, not significant.

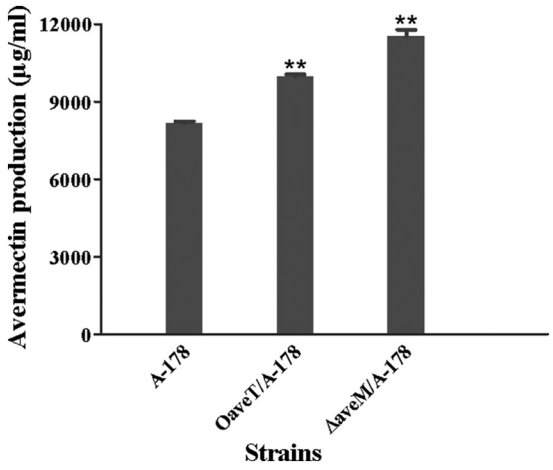

FIG 8 Effects of *aveT* overexpression and *aveM* deletion on avermectin production in industrial strain A-178. OaveT/A-178, an *aveT*-overexpressing strain of A-178; ΔaveM/A-178, an *aveM* deletion strain of A-178. **, $P < 0.01$ by Student's *t* test.

overexpressing strain OaveM displayed delayed aerial hypha formation and sporulation on YMS and MM media (see Fig. S6 in the supplemental material), indicating that *aveM* has a negative effect on morphological differentiation. These findings are consistent with those for the phenotype, the avermectin production level, and the *aveM* transcription level in strains ΔaveT and OaveT, suggesting that AveT regulates avermectin production and morphological differentiation primarily by repressing *aveM* transcription.

Overexpression of *aveT* and deletion of *aveM* increase avermectin production in an industrial strain. The *aveT* transcription level in industrial strain A-178 was higher than that in the WT strain, whereas *aveM* expression was lower in A-178 (see Fig. S7 in the supplemental material), consistent with the high avermectin yield in A-178. To investigate the possible improvement of avermectin production in A-178 by engineering of *aveT* and *aveM*, we introduced *aveT*-overexpressing vector pKC1139-ermp-aveT and *aveM* gene deletion vector pΔaveM into A-178 to construct mutants OaveT/A-178 and ΔaveM/A-178, respectively. In comparison with the level of avermectin production in parental strain A-178, the level of avermectin production was increased ~22% in OaveT/A-178 and ~42% in ΔaveM/A-178 (Fig. 8). Thus, *aveT* overexpression and *aveM* deletion appear to be effective strategies for further enhancing avermectin production in industrial strains.

Avermectin intermediate C-5–O-B1 affects the DNA-binding activity of AveT. TFRs typically regulate transcription through the ligand-mediated reduction of DNA binding (21). Because TFR ligands are often related to the gene(s) regulated and the important AveT target *aveM* encodes a putative transmembrane efflux protein, it is possible that AveM pumps out the ligand(s) of AveT during fermentation. Kitani et al. (8) found that a novel type of signaling molecule from *S. avermitilis*, termed "avenolide," acts as an autoregulator to elicit avermectin production and that the *aco* (*sav_3706*) gene product (an acyl coenzyme A oxidase) is essential for avenolide biosynthesis. Another possibility is that avenolide acts as an AveT ligand. To test these ideas, we evaluated the effect of concentrated culture supernatant from WT strain ATCC 31267 grown in FM-I on the affinity of AveT for the *aveM-sav_7491* intergenic region by EMSAs. The DNA-binding ability of AveT was inhibited by the presence of WT fermentation broth in a concentration-dependent manner (Fig. 9A), suggesting that the small extracellular molecule(s) produced by *S. avermitilis* acts as a ligand(s) of AveT. To investigate whether AveM pumps out the AveT ligand(s) directly, various amounts of concentrated fermentation broth of the WT strain and strain ΔaveM were added separately to EMSA mixtures. The two broths did not display notable differences in their abilities to abolish the retarded signal of the AveT-DNA complex (see Fig. S8 in the supplemental material), suggesting that the substrate of AveM is not the ligand of AveT. To determine whether avenolide can act as an AveT ligand, we constructed *aco* gene deletion mutant Δaco, which is unable to biosynthesize avenolide and therefore has a greatly reduced avermectin yield. EMSAs were performed using con-

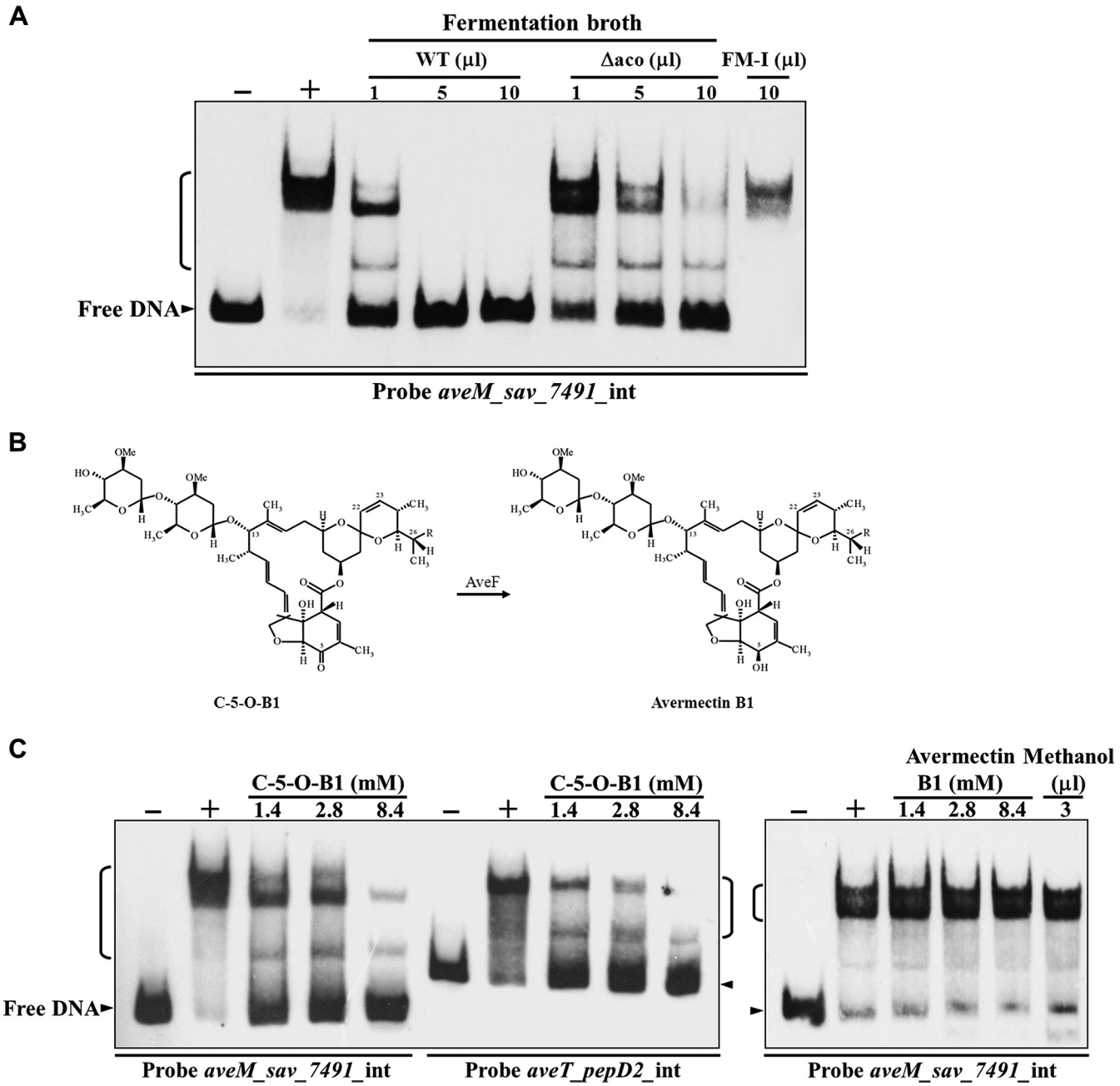

FIG 9 Effect of C-5–O-B1 on AveT binding to target promoter regions. (A) EMSAs of His_6-AveT (0.05 μM) with concentrated fermentation broth of WT and *aco* deletion mutant Δaco grown in FM-I for 10 days. The concentrated supernatant of fermentation medium FM-I was used as a medium control. (B) Structures of C-5–O-B1 and avermectin B1. The conversion of C-5–O-B1 to avermectin B1 is catalyzed by AveF, which reduces the keto group at position C-5 of C-5–O-B1 to a hydroxyl group. (C) EMSAs of His_6-AveT (0.05 μM) with C-5–O-B1 and avermectin B1. Lanes −, control reaction without protein; lanes +, EMSA reaction in the presence of protein. Avermectin and C-5–O-B1 were dissolved in methanol, and methanol was used as a solvent control. In all EMSAs, each reaction mixture contained 0.15 nM labeled probe.

centrated Δaco fermentation broth. The broth inhibited the binding of AveT to probe *aveM_sav_7491*_int. However, this inhibitory effect was much weaker than that of WT fermentation broth (Fig. 9A), suggesting that avenolide is not the AveT ligand and that avermectin and/or its intermediates may be specifically recognized by AveT.

We next performed EMSAs using avermectin B1 and its precursor, C-5–O-B1 (which differs from avermectin B1 in lacking an H at C-5) (Fig. 9B). Avermectin B1 did not induce the dissociation of AveT from probe *aveM_sav_7491*_int even at a concentration of 8.4 mM. Surprisingly, C-5–O-B1 was able to disrupt the AveT-DNA interaction at a concentration of 1.4 mM (Fig. 9C), suggesting that C-5–O-B1 is an AveT ligand and that the hydroxyl (—OH) group at C-5 may abolish the affinity of avermectin B1 for AveT.

Our findings indicate that AveT binds directly to the *aveT*-

pepD2 and *aveM-sav_7491* intergenic regions. To assess the interactions between AveT and these targets in response to C-5–O-B1, we compared the dissociation of AveT from these promoter regions by EMSAs. When the concentrations of AveT and the probes were kept constant, the dissociation of AveT from the two probes with increasing C-5–O-B1 concentration was nearly identical (Fig. 9C). Thus, C-5–O-B1 apparently has no preference in disrupting the interaction of AveT with target DNA regions.

DISCUSSION

In this study, we characterized a novel TFR, AveT, in *S. avermitilis* and demonstrated that it functions as a strong activator of avermectin production and morphological differentiation by regulating the transcription of its target genes. Transcription and EMSAs showed that AveT stimulates avermectin production by altering the transcription of the cluster-situated activator gene *aveR*. This stimulatory effect is indirect, and the upstream regulatory mechanism of *aveR* expression in *S. avermitilis* remains unknown. The direct regulators of *aveR* are being characterized in our ongoing studies, for a better understanding of the regulatory network of avermectin production.

Many TFR genes are oriented divergently to neighboring genes; the degree of divergent orientation is ~50% in *B. subtilis* and >65% in most other bacterial species (18). The situation for *aveT* (*sav_3619*) and *pepD2* (*sav_3620*) is similar. The TetR family is named after the TetR protein, its most completely characterized member. The *tetR* gene is adjacent to and oriented divergently to *tetA*. The transcription of both genes is tightly controlled by TetR through binding to their intergenic region (19). Based on the known TetR mechanism, we found that AveT repressed the transcription of its own gene and *pepD2* by binding to the 18-bp palindromic sequence CGAAACGGTTTCGTTTCG in the *aveT-pepD2* intergenic region. The same inverted repeats were found in the bidirectional *aveM-sav_7491* promoter region. AveT also directly repressed the transcription of *aveM* and *sav_7491*. Similar palindromic sequences were identified in some other promoter regions. Although AveT did not bind to any of the selected putative target sites, we cannot rule out the possibility that it may bind to other similar sequences. Other putative target sites should be further investigated. Further experiments using chromatin immunoprecipitation sequencing will help identify additional AveT target genes, whose functions in *S. avermitilis* can then be investigated.

Four AveT target genes were identified in this study: *aveT*, *pepD2*, *aveM*, and *sav_7491*. Overexpression of *aveT* in both WT and industrial strains increased the level of avermectin production, indicating that the amount of endogenous AveT is not saturating and that enhancement of *aveT* expression is a practical approach to increase avermectin production. The fact that *aveT* is negatively autoregulated suggests that AveT adopts this strategy to strictly control its expression level and avermectin production. *pepD2* encodes a putative tricorn core peptidase. HPLC analysis of avermectin production in *pepD2*-overexpressing strains indicated that *pepD2* does not affect avermectin biosynthesis. Most of the peptides generated by proteasomes and related systems must be degraded to single amino acids to be further used in cell metabolism and for the synthesis of new proteins. Tricorn peptidase works downstream from proteasomes and degrades polypeptides into di- and tripeptides (39). AveT may affect protein degradation by repressing the transcription of *pepD2*.

aveM encodes a transmembrane efflux protein belonging to the MFS and was found to be a primary target of AveT. Despite a lack of sequence similarity, MFS transporters share an MFS fold that contains four structural repeats, each comprising three consecutive transmembrane segments (TMs). All known MFS transporters appear to function as a monomer (40). TFR ligands, as epitomized by the TetR protein, are often related to the genes regulated (18, 20). We therefore investigated the role of *aveM* in transporting the AveT ligand and found that the AveT ligand is not the substrate of AveM. The MFS transport system was originally believed to function primarily in sugar uptake (41), and AveM is predicted to be a sugar (and other molecule) transporter in the annotation of the *S. avermitilis* genome. To evaluate the possible involvement of AveM in sugar uptake, we performed single-carbon-source experiments using a plate assay. The WT, ΔaveM, and OaveM strains showed no detectable change in morphogenesis when grown on MM medium containing D-mannitol, sucrose, glycerol, xylose, glucose, lactose, mannose, fructose, or rhamnose as a sole carbon source. OaveM displayed faster growth than WT and ΔaveM on galactose-containing medium, suggesting that *aveM* may be involved in galactose transport (see Fig. S9 in the supplemental material). In *S. avermitilis*, two L-oleandrose units, a deficiency of which results in a striking decrease in avermectin activity, are involved in the avermectin biosynthetic pathway (42). Although *aveM* maintains a basal expression level in the WT strain, its deletion leads to a significant increase in the level of avermectin production in both WT and industrial strains, indicating that this gene plays an important role in avermectin production. AveM may therefore have some relationship with oleandrose, perhaps pumping out this deoxysugar or its precursors during avermectin biosynthesis. Subsequent studies revealed that the MFS is far more widespread in nature and far more diverse in function than previously thought. Pao et al. (43) divided the members of the MFS known at that time into 17 families, each of which recognizes and transports a distinct class of structurally related compounds. Another possibility is that AveM is involved in expulsion of some other precursor(s) needed for avermectin biosynthesis. AveM is also predicted to be a fungal trichothecene efflux pump (TRI12) in the *S. avermitilis* genome database and has a high level of identity (85 to 89%) with the puromycin resistance protein Pur8 in several *Streptomyces* species, according to BLASTP searches of the NCBI database. *aveM* may therefore be involved in drug efflux and have an effect on drug resistance.

sav_7491 encodes a hypothetical protein with an unknown function. We did not investigate the relationship of this gene with avermectin biosynthesis. The results of fermentation experiments using strain ΔaveTaveM suggest that another AveT target gene(s) besides *aveM* is involved in avermectin biosynthesis. The function of *sav_7491* may therefore be related to avermectin biosynthesis and requires further detailed investigation.

The DNA-binding activity of TFRs is allosterically inactivated by binding of low-molecular-weight ligands in most cases (21). Intermediates or end products of antibiotic biosynthetic pathways have been reported to act as TFR ligands and to affect antibiotic production and export. For example, during production of the aromatic polyketides daunorubicin and doxorubicin in *S. peucetius*, the intermediate rhodomycin D binds to the TFR DnrO to block its self-repression and thereby enhance end production (44). During actinorhodin biosynthesis in *S. coelicolor*, repression by the TFR ActR of the efflux-encoding gene *actAB* is blocked by

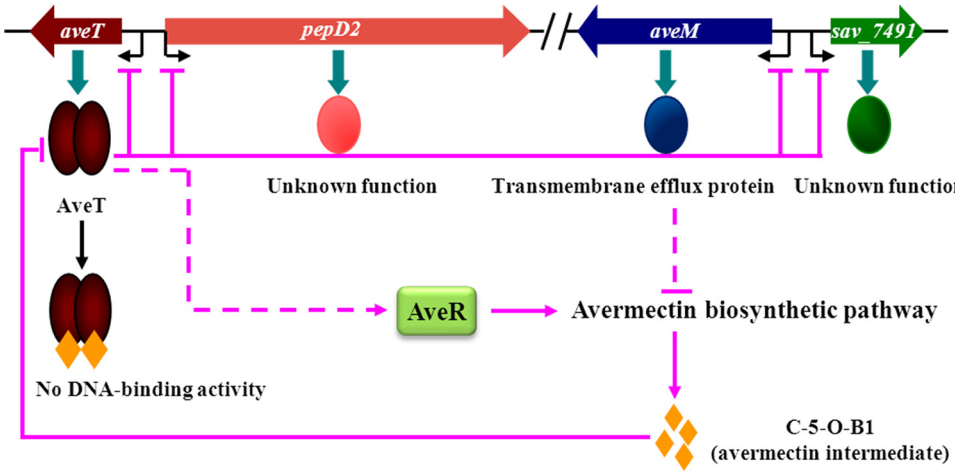

FIG 10 Proposed model of AveT-mediated regulation of avermectin production in *S. avermitilis*. Pink arrows, activation; pink bars, repression; pink solid lines, direct control; pink dashed lines, unknown route.

actinorhodin and the intermediate 4-dihydro-9-hydroxy-1-methyl-10-oxo-3-*H*-naphtho-[2,3-*c*]-pyran-3-(*S*)-acetic acid [(*S*)-DNPA] (45). A similar autoregulatory mechanism was recently reported in which jadomycin B biosynthetic intermediates DHR (dehydrorabelomycin) and DHU (2,3-dehydro-UWM6) bind to its CSR, JadR* (a TFR); affect its binding activity; and ultimately, alter the cofactor supply for jadomycin biosynthesis (46). The results of the present study demonstrate that AveT is dissociated from its target promoters by the late pathway intermediate C-5–O-B1 but not by the end product, avermectin B1. The structure of C-5–O-B1, in comparison with the structure of avermectin B1, lacks only an H at C-5. However, the two compounds display striking differences in hydrophobic properties and polarity. The C-5 keto group may therefore play an essential role in interactions of AveT with its ligand(s). This study was focused primarily on one precursor. Other intermediates besides C-5–O-B1 that have a C-5 keto group are present in the avermectin biosynthetic pathway and may also bind to AveT. The effects on AveT DNA binding of other antibiotics (oligomycin, apramycin, kanamycin, tetracycline, ampicillin, chloramphenicol, streptomycin, thiostrepton, bacitracin) were tested by EMSAs using probe *aveM_sav_7491*_int. None of these antibiotics disrupted the AveT-DNA interaction even at concentrations as high as 8.4 mM (data not shown), suggesting that only an avermectin intermediate(s) acts as an AveT ligand.

Based on the present findings, we propose a model of regulation of avermectin production by AveT and its ligand in *S. avermitilis* (Fig. 10). According to this model, the basal expression level of AveT during early growth of *S. avermitilis* directly represses the transcription of *aveT*, *pepD2*, *aveM*, and *sav_7491* by binding to their promoter regions. When the concentration of the signaling molecule avenolide reaches a certain threshold level, it triggers avermectin production and the subsequent accumulation of C-5–O-B1. When accumulated C-5–O-B1 reaches a threshold level, it is sensed by AveT, resulting in the dissociation of AveT from the target promoters and reversal of the repression of *aveT*, *pepD2*, *aveM*, and *sav_7491*. A high level of AveT theoretically enhances *aveR* expression, which is required for avermectin production. As the level of AveT expression increases, the transcription of the four target genes is again repressed, resulting in appropriate gene expression levels. This scenario is consistent with the *aveT* transcription profile shown in Fig. 3A. AveT and AveM have opposing effects on avermectin production, and the other transcriptional regulators affect *aveR* expression (27, 28, 47), resulting jointly in a gradual increase in the level of avermectin production in cells. The present finding that a late intermediate in the avermectin pathway acts as a regulator of its own production suggests a positive-feedback regulatory mechanism that ensures the irreversible production of avermectins and their appropriate concentration in cells.

It appears that avermectin production in industrial strain A-178, which produces high levels of avermectin, can be enhanced through the manipulation of *aveT* and *aveM* gene expression, providing a useful basis for the rational construction of avermectin overproducers. The present findings are significant to clarify the complex regulatory mechanisms of avermectin biosynthesis and avermectin fermentation by industrial strains producing high levels of avermectin. AveT homologs are highly conserved in the genus *Streptomyces*. Our suggested strategy for improved avermectin production based on engineering of AveT and its target gene(s) may therefore be extended to the enhancement of antibiotic production by other commercially and industrially important *Streptomyces* strains that have AveT homologs.

ACKNOWLEDGMENTS

This study was supported by a grant (no. 31170045) from the National Natural Science Foundation of China.

We are grateful to S. Anderson for English editing of the manuscript.

REFERENCES

1. **Challis GL, Hopwood DA.** 2003. Synergy and contingency as driving forces for the evolution of multiple secondary metabolite production by *Streptomyces* species. Proc Natl Acad Sci U S A **100:**14555–14561. http://dx.doi.org/10.1073/pnas.1934677100.
2. **Bibb MJ.** 2005. Regulation of secondary metabolism in streptomycetes. Curr Opin Microbiol **8:**208–215. http://dx.doi.org/10.1016/j.mib.2005.02.016.
3. **Liu G, Chater KF, Chandra G, Niu GQ, Tan HR.** 2013. Molecular regulation of antibiotic biosynthesis in *Streptomyces*. Microbiol Mol Biol Rev **77:**112–143. http://dx.doi.org/10.1128/MMBR.00054-12.
4. **van Wezel GP, McDowall KJ.** 2011. The regulation of the secondary metabolism of *Streptomyces*: new links and experimental advances. Nat Prod Rep **28:**1311–1333. http://dx.doi.org/10.1039/c1np00003a.

5. **Burg RW, Miller BM, Baker EE, Birnbaum J, Currie SA, Hartman R, Kong YL, Monaghan RL, Olson G, Putter I, Tunac JB, Wallick H, Stapley EO, Oiwa R, Omura S.** 1979. Avermectins, new family of potent anthelmintic agents: producing organism and fermentation. Antimicrob Agents Chemother **15:**361–367. http://dx.doi.org/10.1128/AAC.15.3.361.
6. **Ikeda H, Omura S.** 1997. Avermectin biosynthesis. Chem Rev **97:**2591–2610. http://dx.doi.org/10.1021/cr960023p.
7. **Egerton JR, Ostlind DA, Blair LS, Eary CH, Suhayda D, Cifelli S, Riek RF, Campbell WC.** 1979. Avermectins, new family of potent anthelmintic agents: efficacy of the B1a component. Antimicrob Agents Chemother **15:**372–378. http://dx.doi.org/10.1128/AAC.15.3.372.
8. **Kitani S, Miyamoto KT, Takamatsu S, Herawati E, Iguchi H, Nishitomi K, Uchida M, Nagamitsu T, Omura S, Ikeda H, Nihira T.** 2011. Avenolide, a *Streptomyces* hormone controlling antibiotic production in *Streptomyces avermitilis*. Proc Natl Acad Sci U S A **108:**16410–16415. http://dx.doi.org/10.1073/pnas.1113908108.
9. **Omura S, Ikeda H, Ishikawa J, Hanamoto A, Takahashi C, Shinose M, Takahashi Y, Horikawa H, Nakazawa H, Osonoe T, Kikuchi H, Shiba T, Sakaki Y, Hattori M.** 2001. Genome sequence of an industrial microorganism *Streptomyces avermitilis*: deducing the ability of producing secondary metabolites. Proc Natl Acad Sci U S A **98:**12215–12220. http://dx.doi.org/10.1073/pnas.211433198.
10. **Guo J, Zhao J, Li L, Chen Z, Wen Y, Li J.** 2010. The pathway-specific regulator AveR from *Streptomyces avermitilis* positively regulates avermectin production while it negatively affects oligomycin biosynthesis. Mol Genet Genomics **283:**123–133. http://dx.doi.org/10.1007/s00438-009-0502-2.
11. **Kitani S, Ikeda H, Sakamoto T, Noguchi S, Nihira T.** 2009. Characterization of a regulatory gene, *aveR*, for the biosynthesis of avermectin in *Streptomyces avermitilis*. Appl Microbiol Biotechnol **82:**1089–1096. http://dx.doi.org/10.1007/s00253-008-1850-2.
12. **Aramaki H, Yagi N, Suzuki M.** 1995. Residues important for the function of a multihelical DNA binding domain in the new transcription factor family of Cam and Tet repressors. Protein Eng **8:**1259–1266. http://dx.doi.org/10.1093/protein/8.12.1259.
13. **Fuqua WC, Winans SC, Greenberg EP.** 1994. Quorum sensing in bacteria: the LuxR-LuxI family of cell density-responsive transcriptional regulators. J Bacteriol **176:**269.
14. **Schell MA.** 1993. Molecular biology of the LysR family of transcriptional regulators. Annu Rev Microbiol **47:**597–626. http://dx.doi.org/10.1146/annurev.mi.47.100193.003121.
15. **Egan SM.** 2002. Growing repertoire of AraC/XylS activators. J Bacteriol **184:**5529–5532. http://dx.doi.org/10.1128/JB.184.20.5529-5532.2002.
16. **Weickert MJ, Adhya S.** 1992. A family of bacterial regulators homologous to Gal and Lac repressors. J Biol Chem **267:**15869–15874.
17. **Seoane AS, Levy SB.** 1995. Characterization of MarR, the repressor of the multiple antibiotic resistance *mar* operon in *Escherichia coli*. J Bacteriol **177:**3414–3419.
18. **Ahn SK, Cuthbertson L, Nodwell JR.** 2012. Genome context as a predictive tool for identifying regulatory targets of the TetR family transcriptional regulators. PLoS One **7:**e50562. http://dx.doi.org/10.1371/journal.pone.0050562.
19. **Ramos JL, Martínez-Bueno M, Molina-Henares AJ, Terán W, Watanabe K, Zhang X, Gallegos MT, Brennan R, Tobes R.** 2005. The TetR family of transcriptional repressors. Microbiol Mol Biol Rev **69:**326–356. http://dx.doi.org/10.1128/MMBR.69.2.326-356.2005.
20. **Corre C.** 2013. In search of the missing ligands for TetR family regulators. Chem Biol **20:**140–142. http://dx.doi.org/10.1016/j.chembiol.2013.02.005.
21. **Yu Z, Reichheld SE, Savchenko A, Parkinson J, Davidson AR.** 2010. A comprehensive analysis of structural and sequence conservation in the TetR family transcriptional regulators. J Mol Biol **400:**847–864. http://dx.doi.org/10.1016/j.jmb.2010.05.062.
22. **Hu B, Lidstrom M.** 2012. CcrR, a TetR family transcriptional regulator, activates the transcription of a gene of the ethylmalonyl coenzyme A pathway in *Methylobacterium extorquens* AM1. J Bacteriol **194:**2802–2808. http://dx.doi.org/10.1128/JB.00061-12.
23. **Miyamoto KT, Kitani S, Komatsu M, Ikeda H, Nihira T.** 2011. The autoregulator receptor homologue AvaR3 plays a regulatory role in antibiotic production, mycelial aggregation and colony development of *Streptomyces avermitilis*. Microbiology **157:**2266–2275. http://dx.doi.org/10.1099/mic.0.048371-0.
24. **Uguru GC, Stephens KE, Stead JA, Towle JE, Baumberg S, McDowall KJ.** 2005. Transcriptional activation of the pathway-specific regulator of the actinorhodin biosynthetic genes in *Streptomyces coelicolor*. Mol Microbiol **58:**131–150. http://dx.doi.org/10.1111/j.1365-2958.2005.04817.x.
25. **Chattoraj P, Mohapatra SS, Rao JL, Biswas I.** 2011. Regulation of transcription by SMU.1349, a TetR family regulator, in *Streptococcus mutans*. J Bacteriol **193:**6605–6613. http://dx.doi.org/10.1128/JB.06122-11.
26. **He F, Liu W, Sun D, Luo S, Chen Z, Wen Y, Li J.** 2014. Engineering of the TetR family transcriptional regulator SAV151 and its target genes increases avermectin production in *Streptomyces avermitilis*. Appl Microbiol Biotechnol **98:**399–409. http://dx.doi.org/10.1007/s00253-013-5348-1.
27. **Guo J, Zhang X, Luo S, He F, Chen Z, Wen Y, Li J.** 2013. A novel TetR family transcriptional regulator, SAV576, negatively controls avermectin biosynthesis in *Streptomyces avermitilis*. PLoS One **8:**e71330. http://dx.doi.org/10.1371/journal.pone.0071330.
28. **Guo J, Zhang X, Chen Z, Wen Y, Li J.** 2014. Two adjacent and similar TetR family transcriptional regulator genes, *SAV577* and *SAV576*, coregulate avermectin production in *Streptomyces avermitilis*. PLoS One **9:**e99224. http://dx.doi.org/10.1371/journal.pone.0099224.
29. **Liu Y, Yan T, Jiang L, Wen Y, Song Y, Chen Z, Li J.** 2013. Characterization of SAV7471, a TetR-family transcriptional regulator involved in the regulation of coenzyme A metabolism in *Streptomyces avermitilis*. J Bacteriol **195:**4365–4372. http://dx.doi.org/10.1128/JB.00716-13.
30. **Duong CT, Lee HN, Choi SS, Lee SY, Kim ES.** 2009. Functional expression of *SAV3818*, a putative TetR-family transcriptional regulatory gene from *Streptomyces avermitilis*, stimulates antibiotic production in *Streptomyces* species. J Microbiol Biotechnol **19:**136–139. http://dx.doi.org/10.4014/jmb.0806.387.
31. **Ikeda H, Kotaki H, Tanaka H, Omura S.** 1988. Involvement of glucose catabolism in avermectin production by *Streptomyces avermitilis*. Antimicrob Agents Chemother **32:**282–284. http://dx.doi.org/10.1128/AAC.32.2.282.
32. **Kieser T, Bibb MJ, Buttner MJ, Chater KF, Hopwood DA.** 2000. Practical *Streptomyces* genetics: a laboratory manual. John Innes Foundation, Norwich, United Kingdom.
33. **MacNeil DJ, Klapko LM.** 1987. Transformation of *Streptomyces avermitilis* by plasmid DNA. J Ind Microbiol **2:**209–218. http://dx.doi.org/10.1007/BF01569542.
34. **Chen Z, Wen J, Song Y, Wen Y, Li J.** 2007. Enhancement and selective production of avermectin B by recombinants of *Streptomyces avermitilis* via intraspecific protoplast fusion. Chin Sci Bull **52:**616–622. http://dx.doi.org/10.1007/s11434-007-0119-y.
35. **Zhao J, Wen Y, Chen Z, Song Y, Li J.** 2007. An *adpA* homologue in *Streptomyces avermitilis* is involved in regulation of morphogenesis and melanogenesis. Chin Sci Bull **52:**623–630. http://dx.doi.org/10.1007/s11434-007-0105-4.
36. **Zianni M, Tessanne K, Merighi M, Laguna R, Tabita FR.** 2006. Identification of the DNA bases of a DNase I footprint by the use of dye primer sequencing on an automated capillary DNA analysis instrument. J Biomol Tech **17:**103.
37. **Romero DA, Hasan AH, Lin YF, Kime L, Ruiz-Larrabeiti O, Urem M, Bucca G, Mamanova L, Laing EE, Wezel GP, Smith CP, Kaberdin VR, McDowall KJ.** 2014. A comparison of key aspects of gene regulation in *Streptomyces coelicolor* and *Escherichia coli* using nucleotide-resolution transcription maps produced in parallel by global and differential RNA sequencing. Mol Microbiol **94:**963–987. http://dx.doi.org/10.1111/mmi.12810.
38. **Zheng X, Hu GQ, She ZS, Zhu H.** 2011. Leaderless genes in bacteria: clue to the evolution of translation initiation mechanisms in prokaryotes. BMC Genomics **12:**361. http://dx.doi.org/10.1186/1471-2164-12-361.
39. **Groll M, Bochtler M, Brandstetter H, Clausen T, Huber R.** 2005. Molecular machines for protein degradation. Chembiochem **6:**222–256. http://dx.doi.org/10.1002/cbic.200400313.
40. **Shi Y.** 2013. Common folds and transport mechanisms of secondary active transporters. Annu Rev Biophys **42:**51–72. http://dx.doi.org/10.1146/annurev-biophys-083012-130429.
41. **Maiden MC, Davis EO, Baldwin SA, Moore DC, Henderson PJ.** 1987. Mammalian and bacterial sugar transport proteins are homologous. Nature **325:**641–643. http://dx.doi.org/10.1038/325641a0.
42. **Wohlert S, Lomovskaya N, Kulowski K, Fonstein L, Occi JL, Gewain KM, MacNeil DJ, Hutchinson CR.** 2001. Insights about the biosynthesis of the avermectin deoxysugar L-oleandrose through heterologous expression of *Streptomyces avermitilis* deoxysugar genes in *Streptomyces lividans*. Chem Biol **8:**681–700. http://dx.doi.org/10.1016/S1074-5521(01)00043-6.

43. **Pao SS, Paulsen IT, Saier MH.** 1998. Major facilitator superfamily. Microbiol Mol Biol Rev **62:**1–34.
44. **Jiang H, Hutchinson CR.** 2006. Feedback regulation of doxorubicin biosynthesis in *Streptomyces peucetius*. Res Microbiol **157:**666–674. http://dx.doi.org/10.1016/j.resmic.2006.02.004.
45. **Tahlan K, Ahn SK, Sing A, Bodnaruk TD, Willems AR, Davidson AR, Nodwell JR.** 2007. Initiation of actinorhodin export in *Streptomyces coelicolor*. Mol Microbiol **63:**951–961. http://dx.doi.org/10.1111/j.1365-2958.2006.05559.x.
46. **Zhang Y, Pan G, Zou Z, Fan K, Yang K, Tan H.** 2013. JadR*-mediated feed-forward regulation of cofactor supply in jadomycin biosynthesis. Mol Microbiol **90:**884–897. http://dx.doi.org/10.1111/mmi.12406.
47. **Luo S, Sun D, Zhu J, Chen Z, Wen Y, Li J.** 2014. An extracytoplasmic function sigma factor, σ^{25}, differentially regulates avermectin and oligomycin biosynthesis in *Streptomyces avermitilis*. Appl Microbiol Biotechnol **98:**7097–7112. http://dx.doi.org/10.1007/s00253-014-5759-7.
48. **Bierman M, Logan R, O'Brien K, Seno ET, Rao RN, Schoner BE.** 1992. Plasmid cloning vectors for the conjugal transfer of DNA from *Escherichia coli* to *Streptomyces* spp. Gene **116:**43–49. http://dx.doi.org/10.1016/0378-1119(92)90627-2.
49. **Li L, Guo J, Wen Y, Chen Z, Song Y, Li J.** 2010. Overexpression of ribosome recycling factor causes increased production of avermectin in *Streptomyces avermitilis* strains. J Ind Microbiol Biotechnol **37:**673–679. http://dx.doi.org/10.1007/s10295-010-0710-0.